

LIST OF PUBLICATIONS

1. 'Evolution of Electrospinning in Liver Tissue Engineering' **Vasudevan, A.**, Tripathi, D. M., Sundarajan, S., Venugopal, J. R., Ramakrishna, S., & Kaur, S. (2022). Evolution of Electrospinning in Liver Tissue Engineering. *Biomimetics*, 7(4), 149.

<https://doi.org/10.3390/biomimetics7040149>

I.F (3.74) **Citations= 6**

2. Kaur S, Kaur I, Rawal P, Tripathi DM, **Vasudevan A.** Non-matrigel scaffolds for organoid cultures. *Cancer Lett.* 2021;504:58-66.

<http://dx.doi.org/10.1016/j.canlet.2021.01.025>

I.F (9.7) **Citations= 41**

3. Primary Hepatocyte Isolation and Cultures: Technical Aspects, Challenges and Advancements. Kaur I, **Vasudevan A.**, Kaur S, Rawal P, Tripathi DM, January 2023, *Bioengineering*10(2):131.

[10.3390/bioengineering10020131](https://doi.org/10.3390/bioengineering10020131).

I.F (5) **Citations= 1**

4. Chemically Modified Dipeptide Based Hydrogel Supports Three-Dimensional Growth and Functions of Primary Hepatocytes. S Biswas, **Vasudevan A.**, N Yadav, P Rawal, I Kaur, Tripathi DM, Kaur S. August 2022. *ACS Applied Bio Materials*.

DOI: [10.1021/acsabm.2c00526](https://doi.org/10.1021/acsabm.2c00526).

I.F (3.25) **Citations= 3**

5. *Mangifera indica* and *Mangifera zeylanica*: Perspectives on medicinal properties, therapeutic applications and potential uses as anticancer epigenetic drugs. I Selvakumar, **Vasudevan A.**, P Nirmal. February 2022.

DOI: [10.3892/ije.2022.10](https://doi.org/10.3892/ije.2022.10)

I.F (4.86) **Citations= 2**

6. Ashwin V, Nilotpal M and et al., **Liver Extracellular matrix-based Nanofiber scaffolds for the culture of primary hepatocytes and drug screening'**

(Under Revision ACS Biomaterial science and engineering)



Review

Evolution of Electrospinning in Liver Tissue Engineering

Ashwini Vasudevan ¹, Dinesh M. Tripathi ¹, Subramanian Sundarrajan ², Jayarama Reddy Venugopal ³, Seeram Ramakrishna ² and Savneet Kaur ^{1,*}

¹ Department of Molecular and Cellular Medicine, Institute of Liver and Biliary Sciences, New Delhi 110070, India

² Department of Mechanical Engineering, National University of Singapore, Singapore 117581, Singapore

³ Faculty of Industrial Sciences and Technology, Universiti Malaysia Pahang, Pekan 26600, Malaysia

* Correspondence: savykaur@gmail.com

Abstract: The major goal of liver tissue engineering is to reproduce the phenotype and functions of liver cells, especially primary hepatocytes *ex vivo*. Several strategies have been explored in the recent past for culturing the liver cells in the most apt environment using biological scaffolds supporting hepatocyte growth and differentiation. Nanofibrous scaffolds have been widely used in the field of tissue engineering for their increased surface-to-volume ratio and increased porosity, and their close resemblance with the native tissue extracellular matrix (ECM) environment. Electrospinning is one of the most preferred techniques to produce nanofiber scaffolds. In the current review, we have discussed the various technical aspects of electrospinning that have been employed for scaffold development for different types of liver cells. We have highlighted the use of synthetic and natural electrospun polymers along with liver ECM in the fabrication of these scaffolds. We have also described novel strategies that include modifications, such as galactosylation, matrix protein incorporation, etc., in the electrospun scaffolds that have evolved to support the long-term growth and viability of the primary hepatocytes.



Citation: Vasudevan, A.; Tripathi, D.M.; Sundarrajan, S.; Venugopal, J.R.; Ramakrishna, S.; Kaur, S.

Evolution of Electrospinning in Liver Tissue Engineering. *Biomimetics* **2022**, *7*, 149. <https://doi.org/10.3390/biomimetics7040149>

Academic Editor: Huihua Yuan

Received: 20 August 2022

Accepted: 15 September 2022

Published: 30 September 2022

Publisher's Note: MDPI stays neutral with regard to jurisdictional claims in published maps and institutional affiliations.



Copyright: © 2022 by the authors. Licensee MDPI, Basel, Switzerland. This article is an open access article distributed under the terms and conditions of the Creative Commons Attribution (CC BY) license (<https://creativecommons.org/licenses/by/4.0/>).

Keywords: liver tissue engineering; electrospinning; nanofibers; natural and synthetic polymers; extracellular matrix proteins; hepatocytes

1. Introduction

‘Nanotechnology’ came into existence in the year 1974 and today has advanced in almost all the fields of science, namely, medicine, metals, textiles, waste management, electronics and tissue engineering [1]. Nanotechnology deals with the study of particles less than 100 nm in diameter. Nanoparticles may vary in terms of shape and size and also properties such as optical activity, reactivity and toughness. Due to their high surface area and fine-tunable properties, nanoparticles have achieved widespread success in diverse scientific applications. Nanotechnology has revolutionized the field of tissue engineering by producing biomimetic nanofiber scaffolds. Nanofiber scaffolds are prepared with various types of materials, such as ceramics, metals, natural and synthetic polymers, to create nanofibers and nanopatterns. These scaffolds are now gaining popularity as their biological and topographical properties closely mimic the extracellular matrix (ECM) properties of the tissues [2,3]. Cell–matrix interactions are crucial for the optimal functioning of any tissue and nanofibrous scaffolds can provide this matrix substrate for the adhesion and proliferation of cells. Nanopolymers provide the most appropriate microenvironment for cell growth and are now being used for a plethora of tissue engineering applications including the creation of tissue implants for regenerative medicine, physiological tissue scaffolds for disease modeling, drug screening etc. [4,5]. Several techniques are available to develop nanofibers and nanopatterned structures including electrospinning, particulate leaching, lithography, self-assembly, phase separation and freeze drying (Figure 1).

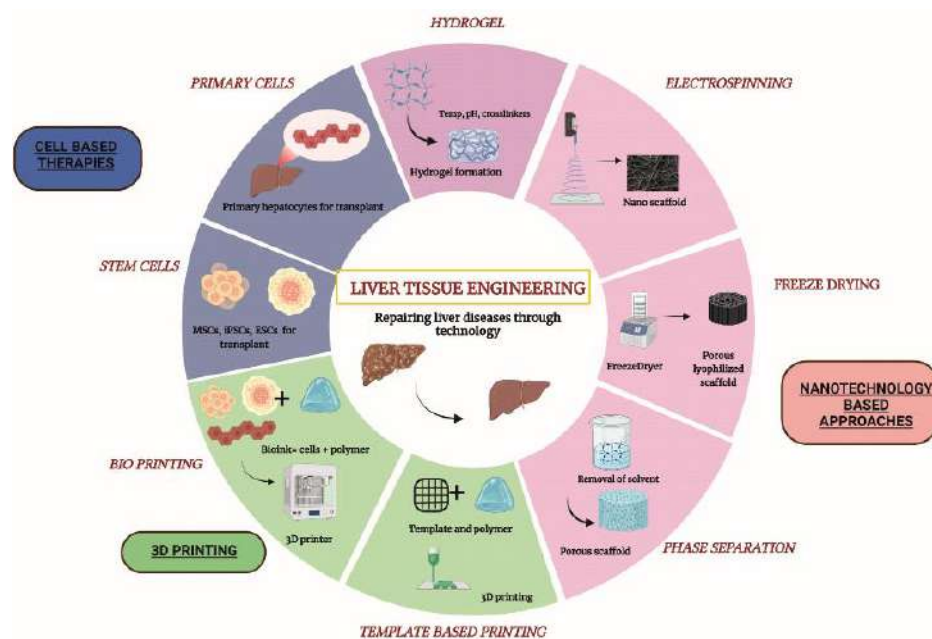


Figure 1. Different approaches used in liver tissue engineering. Three broad areas under liver tissue engineering categorized as cell-based approaches, 3D printing and nanotechnology-based approaches. MSCs—Mesenchymal Stem cells; iPSCs—induced pluripotent stem cells; ESCs—Embryonic Stem Cells. (Unpublished original picture by authors created using Biorender.com).

Electrospinning is preferred over the other scaffold fabrication techniques because the pore size can be controlled in electrospun fibers which cannot be regulated in other techniques, namely, self-assembly and particulate leaching, which produce microporous structures. Electrospinning can fabricate user-defined scaffolds with optimum pore size as per the cell requirement. This technique also allows the development of scaffolds with naturally occurring polymers, such as alginate, gelatin and chitosan, as well as synthetic polymers. Nanofiber scaffolds produced from electrospinning have an orientation that mimics the dense collagen network of the natural ECM. Several studies have also proven that the orientation of the electrospun nanofibers promotes the attachment of cells by providing optimum spacing of integrin binding [6,7]. Electrospun nanofiber scaffolds have thus been widely used in the *in vitro* cultures. Additionally, unlike electrospinning, the rest of the techniques utilize high temperature and corrosive salts and chemicals, which may affect the biocompatibility of the fabricated scaffolds [8–10].

Nanofiber scaffolds produced by the electrospinning technique have been used in all fields of tissue engineering, to name a few, bone, cardiovascular, ligament and skin tissue engineering [11–13]. Aligned nanofibers produced by this technique are highly favorable for the growth of osteocytes. The mechanical stability of these nanofiber scaffolds also provides an added advantage during the *in vivo* transplantation of osteocytes [14–17]. The importance of electrospinning in the field of skin tissue engineering is its ability to fabricate the scaffolds as thin sheets that can be used as a patch to treat topical wounds. With this technique, we can also incorporate specific growth factors in the fabricated scaffolds and attempt adequate surface modifications for improved adhesion of the cultured cells [18].

The liver is the largest organ of the body and is involved in the metabolism of drugs and xenobiotics, detoxification, bile formation and energy synthesis functions. According to a recent study, liver diseases account for about 2 million deaths per year worldwide. Liver transplantation is the only option for patients with end-stage liver failure [19–21]. According to Health Resources and Service Administration (HRSA based in the USA), it has been reported that there has been a 10% increase in patients waiting for a liver transplant during the year 2021 (until September) globally. The list of waiting patients largely outnumbers the list of donor livers and only 1 out of 100 deserving liver disease

patients finally receive a liver. The remaining mostly die with the want of a fully functional liver. Given the increasing burden of patients with end-stage liver diseases and the resulting dearth of suitable donor organs, scientists worldwide have been exploring other options, such as extracorporeal temporary liver assist devices [22–24], tissue engineering approaches, 3D printing and cell-based therapies, to combat liver diseases and most of these have also shown promising results in pre-clinical studies. The fabrication of scaffolds, implantable devices, cell encapsulated hydrogels and 3D printed liver tissues are being investigated under the umbrella of liver tissue engineering [25,26].

In the current review, we review technical aspects of electrospinning, its current use in liver tissue engineering and also its future potential in the field of liver tissue engineering.

2. Electrospinning

The invention of electrospinning dates back to 1980, by Yoshito Miura and group who were working on textile fibers [27], yet the use of electrospinning techniques in the field of tissue engineering to prepare nano-range scaffolds increased only in the past two decades [28]. A major advantage of this technique is that nanofibrous scaffolds with high surface area and porosity can be developed for the exchange of nutrients and oxygen and also allows infiltration of cells within the scaffold [29]. Electrospun fibers are in the nano range (from 100 nm to 50 μ m) and have been observed to mimic the ECM architecture of a biological tissue. Several growth factors and drugs can be incorporated into these electrospun scaffolds through simple chemical modification of the surface [30–36], which can then be used as sustained drug releasing materials *in vivo* owing to their porous nature. Electrospun scaffolds are ideal for *in vitro* cultures and are also now being used for *in vivo* transplantation, especially in vascular reconstruction and skin tissue engineering [37–39]. Advancements in the field of electrospinning have given rise to its various subtypes, including coaxial electrospinning, multiple needle electrospinning, melt electrospinning, wet electrospinning and blend electrospinning. Core-sheath and hollow fibers can be produced by the coaxial spinning type, which has outer and inner spinnerets that can contain two different polymer solutions [40,41]. Blend electrospinning is different from coaxial spinning, where two polymers, or polymers with drugs or growth factors, can be blended and electrospun. Due to the toxicity of the nonpolar solvents used in a conventional electrospinning process, blending may result in the degradation of growth factors and active metabolites in drugs. To overcome this difficulty, two-phase electrospinning, where two different electrospinning methods are combined, is preferred, which allows the stability of growth factors and drugs to be maintained [42,43]. Melt electrospinning does not involve the use of toxic solvents, and, thus, is favorable for both *in vitro* cultures and *in vivo* conditions [44,45]. This process, however, requires very high temperatures to melt the polymer and only very few polymers are stable at high temperatures (e.g.: polycaprolactone and polyethylene). Wet electrospinning is another widely used electrospinning method which produces highly porous scaffolds with better cellular infiltration [46]. Conventional electrospinning systems have also been modified with multiple needles and multiple spinneret systems to fabricate scaffolds on a large scale.

A basic electrospinning set-up comprises of a syringe pump, syringe with blunt needle containing polymer solution, a collector and a high voltage current source. A high-intensity electric field (15 to 30 kV) is applied between two oppositely charged electrodes to set up electrospinning for scaffold production. One electrode is connected to the collector and the other is attached to the needle of the syringe containing the polymer solution. The flow rate at which the polymer solution is ejected out of the syringe pump is optimized according to the user's experiment. The polymer is electrically charged as soon as it comes out of the nozzle as a spherical droplet. A charge–charge repulsion within the droplet creates a surface tension over the droplet, which is overcome by the high intensity electric field drawing the spherical droplet into a cone towards the collector [47]. This is called Taylor cone formation, which is then followed by jet propagation. During jet propagation, solvent evaporation occurs and the charge within the jet increases with time and voltage.

This causes instability of the jet and the fibers become patterned in the nanoscale range, which are then drawn towards the collector. The orientation of the patterned fibers formed depends on the collectors used. For example, the rotating drum collectors lead to the formation of aligned fibers, while static collectors would form random fibers [48] (Figure 2). In case of the wet electrospinning method, the fibers are collected in the water bath and rest of the set-up remains the same. Cell behavior varies drastically according to the surface topography of the electrospun scaffolds. Studies have reported that primary hepatocytes and cells of elongated phenotype-like myocytes and neuronal cells show improved cellular attachment and proliferation when cultured on aligned fibers, while non-elongated cell phenotypes are more proliferative on random fiber mats [49–53]. The seeded cells sense the surface changes through integrin receptor signaling (present on the surface of the cells) and different levels of receptor activation by different scaffolds cause a variability in cell adhesion and attachment.




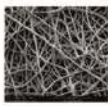



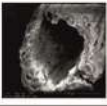
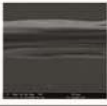
Composition	Natural <ul style="list-style-type: none"> • Collagen • Chitosan • Silk • Alginate 	Synthetic <ul style="list-style-type: none"> • PCL • PLLA • PLGA • PHBV 	Blended <ul style="list-style-type: none"> • Natural+Synthetic • Natural+Synthetic+Coating
Morphology	Solid 	Porous 	Core-shell 
Assembly	Random 	Aligned 	Layered 
	Yarn 	Hollow yarn 	Fiber bundle 

Figure 2. Patterns of the electrospun nanofibers categorized. Nanofibers can be electrospun in different formats such as random, aligned and layered depending on the instrumentation. Figure formatted with permission (NUSNNI, NUS).

Every component of the electrospinning setup can affect the formation of fibers and can also change the range/size at which the fibers are formed [54]. Rahmati et al. categorized various factors affecting fiber formation into three major groups, where the first group revolves around intrinsic properties of the materials used, including majorly the molecular weight of the polymer, viscosity and solvent nature. The molecular weight of the polymer plays a major role in determining the fiber formation and diameter. Increased molecular weight of the polymer increases the viscosity of the electrospinning solution. Highly viscous polymers tend to surpass the bending instability and form fibers with large diameters. The second group involves the processing parameters related to the equipment such as flow rate, distance between the needle and collector and voltage. Improper fiber formation may occur due to inadequate solvent evaporation when the flow rate and the distance are not adjusted. With increased flow rates and decreased distance between the collector and the needle, the solution in which the polymer is dissolved does not get the requisite time to evaporate, due to which a thick fiber mesh with inadequate pore size is formed. Jet propagation and solvent evaporation are thus two crucial factors that determine the fiber formation, which is governed by appropriate flow rates for developing several patterns of the fibers. The third category of factors affecting the electrospinning of fibers accounts for environmental factors such as humidity and temperature. Low temperature and high humidity in the air affect solvent evaporation and lead to improper fiber formation [55,56].

Polymers used for electrospinning of fibers can be natural (such as alginate, chitosan, silk, etc.) or synthetic PLA (polylactic acid), PLGA (polylactic co glycolide), PCL (polycaprolactone) or even both (hybrid polymers) [57,58]. The degradation products of PLA and PLGA polymers (lactic acid) are biocompatible. PCL is known for its non-toxicity and lower immunogenicity and cases where slower degradation of polymer is needed, such as in cases of nerve regeneration through tissue engineering [59]. The degradation products of PCL (caproic acid, succinic acid, valeric acid and butyric acid) have shown to be toxic for cell culture systems, but, surprisingly, PCL implants have been reported to perform well inside the host body [60]. The slow degradation rate of this polymer is the main reason for it to be used widely in drug delivery systems. PCL scaffolds are also porous, which allows improved growth of cells in the in vitro systems and also in vivo. When transplanted in vivo, endothelial cells can infiltrate and form new blood vessels to support angiogenesis and cell viability on PCL scaffolds. It has been reported that electrospinning of natural polymers (collagen, silk fibroin) alone results in a bead on string fiber formation and, hence, natural polymers are often mixed with a synthetic polymer to improve the mechanical properties of the formed fibers [61,62]. Overall, the high surface area of the electrospun scaffolds provide a suitable environment for cellular attachment and the nano size of the fibers that mimics the cellular protein size present in the natural tissue matrix improves the focal adhesion.

3. Hepatic Cell Types on Electrospun Nanofiber Scaffolds

Hepatocytes account for 80% of the hepatic volume and perform all the major functions of liver. The other cell types present in the liver are grouped as non-parenchymal cells (NPC), which mainly includes hepatic stellate cells, kupffer cells, sinusoidal endothelial cells and other cell types such as pit cells and cholangiocytes. NPCs hold for about 6.5% of the total hepatic volume. Sinusoidal endothelial cells are found on the lining of the space of Disse. They are different from the conventional endothelial cells due to the presence of fenestrae that facilitates the improved exchange of nutrients and oxygen. Kupffer cells are the major phagocytic cell type in the liver. Hepatic stellate cells are the reservoir of vitamin A and pit cells are the natural killer cells of the liver. Cholangiocytes are the cells lining the bile ducts [63]. The cellular architecture of the liver is supported by the extracellular matrix (ECM) with an array of several different macromolecules that together comprise the scaffolding of the liver. In a healthy liver, it forms only about 3% of its total area. The most abundant proteins of liver ECM are isotypes of collagen (I, III, IV and V), with different isotypes localized to different areas.

Prolonged cultures of viable and functional liver cells such as primary hepatocytes and hepatoma cell lines on nanofiber scaffolds is the major goal of liver tissue engineering. The survival of primary hepatocytes ex vivo has remained a challenge for years. Adult primary hepatocytes do not survive after 3–4 days of culture as they change their phenotype and transform into mesenchymal cell lineages. The use of electrospun scaffolds for liver tissue engineering was first reported in the 21st century [56–61]. Zhang-Qi Feng et al. were some of the few researchers who pioneered the culturing of liver cells on electrospun scaffolds [60,64,65]. Among the cell lines, HepG2 shows better efficiency when cultured on electrospun fibrous scaffolds, on both natural (silk fibroin) as well as (PCL) synthetic polymer. Other than the hepatoma cell lines, cryopreserved human primary hepatocytes and rat/mice isolated primary hepatocytes have also been cultured on electrospun scaffolds, however, with limited success. It has been observed that primary hepatocytes display better viability with the natural polymers or with synthetic polymer scaffolds when they are modified with matrix proteins such as collagen, fibronectin or RGD peptides [66–71]. Another bottleneck of culturing primary hepatocytes is their limited replicative potential in vitro. An effective approach that has now emerged is to grow these cells as spheroids. Bell et al. have shown that hepatocytes can be cultured as spheroids for up to 35 days without compromising their functionality [70]. Hepatocytes have also been seen to form spheroids when cultured on galactosylated surfaces [71–77]. Galactose–asialoglycoprotein receptor (AS-

GPR) present on the hepatocytes has been demonstrated to be a key player mediating this interaction. Kian-Ngiap Chua et al. used poly (ε-caprolactone-co-ethyl ethylene phosphate) (PCLEEP) polymer for scaffold formation and surface-modified it with polyacrylic acid and -O-(60- aminoethyl)-D-galactopyranoside (AHG) for galactosylation [75]. Isolated rat hepatocytes began to form clusters after day 1 on these galactosylated scaffolds. This was not observed on the non-galactosylated substrate, where the cells took an irregular shape and topography. Functional analysis revealed that an increased secretion of albumin and urea synthesis was observed with hepatocytes cultured on galactosylated substrates after 2 days and P450 activity increased after day 5. This was a major advantage of the developed substrate as it has been reported that P450 activity of primary hepatocytes usually deteriorates with time in culture conditions otherwise [72,73]. Hong-Fang Lu et al. showed that hepatic spheroids co-cultured with non-parenchymal cells on galactosylated PVDF (Polyvinylidene fluoride) surface have enhanced P450 activity [74]. Several other studies also reported the efficiency of galactosylated surfaces in maintaining hepatic spheroid phenotype, function and preventing their trans-differentiation [75–79]. Another study by Kian-Ngiap Chua et al. employed a dual-functional scaffold for facilitating adhesion and enhanced functionality of the primary hepatocyte spheroids. 3-methylcholanthrene (3-Mc) is a selective inducer of P450, and this group prepared 3-Mc-loaded electrospun PCLEEP polymer scaffolds by mixing the inducer with the polymer solution before spinning them into scaffolds. The galactosylated surface helped in the prolonged culture of the hepatocytes as spheroids and the bio-molecule-loaded feature improved the functionality of hepatocytes. Galactosylated scaffolds showed 85% cell adhesion, whereas attachment was a little low with 3-Mc loaded scaffolds (76%) and very poor attachment was observed with the unmodified scaffolds (PCLEEP alone) (37%). The P450 function of the dual scaffolds increased by 1.5-fold in comparison with the galactosylated scaffolds, clearly demonstrating the usefulness of this approach [80]. Besides primary hepatocytes, bone marrow stem cells (BMSCs), human mesenchymal stem cells (hMSCs), etc., have also been used in liver tissue engineering, where these cells are seeded onto the electrospun fibrous scaffolds and are trans-differentiated into hepatocytes with appropriate growth factors. This approach has also extended the life span and functionality of the differentiated hepatocytes in vitro [81–84].

4. Electrospun Synthetic Polymers for Liver Cell Cultures

Synthetic polymers used for liver tissue engineering are PLA, PLLA (Poly-L-Lactic Acid), PCL and PLGA. Figure 3 provides an overview of different polymers and technical electrospinning parameters used in liver tissue engineering. Among the synthetic polymers, PLA and PCL are the most preferred polymers. PLA was one of the first polymers used for tissue engineering applications. Liu and group have recently summarized applications of PLA in tissue engineering [82]. However, PLA alone does not effectively facilitate cellular attachment, thus, PLA is mostly combined with any natural polymer or matrix proteins and used for liver tissue engineering approaches. For example, a combination of PLA composite with silk fibroin has been reported for liver cell lines, HepG2 cells [83]. Liu et al. used lecithin- doped electrospun PLA scaffolds to achieve better cellular viability and functionality of HepG2 cells. Lecithin has been incorporated in this study since PLA lacks the biological component required for the proper attachment of cells. Increased cell viability and the highest cellular activity was observed in the group containing lecithin with PLA after 3 days of culture [67]. Collagen, being the most abundant protein in the matrix, has been widely incorporated with synthetic polymers to support hepatic cells. Hepatic differentiation of hBMSCs(human Bone Marrow derived stem cells) has been observed with scaffolds containing PLLA with collagen [85]. A study by Das et al. has shown that incorporating two majorly present ECM proteins, collagen and fibronectin, in different ratios with PLGA showed improved CYP gene activity of Huh7.5 hepatoma cells. They have employed wet electrospinning to obtain fibers with increased pore size in this study. The cells were cultured for 28 days on the modified scaffold and a tenfold increase in cell number was observed with the scaffold having the collagen to fibronectin protein ratio (C:F)

of 3:1. Enhanced cell death was observed in the group without the ECM proteins (C:F = 0:0). CYP3A4 and CYP3A7 expression were 7.3-fold and 4.5-fold higher in the modified scaffold with the 3:1 ratio when compared to the unmodified scaffolds [46].

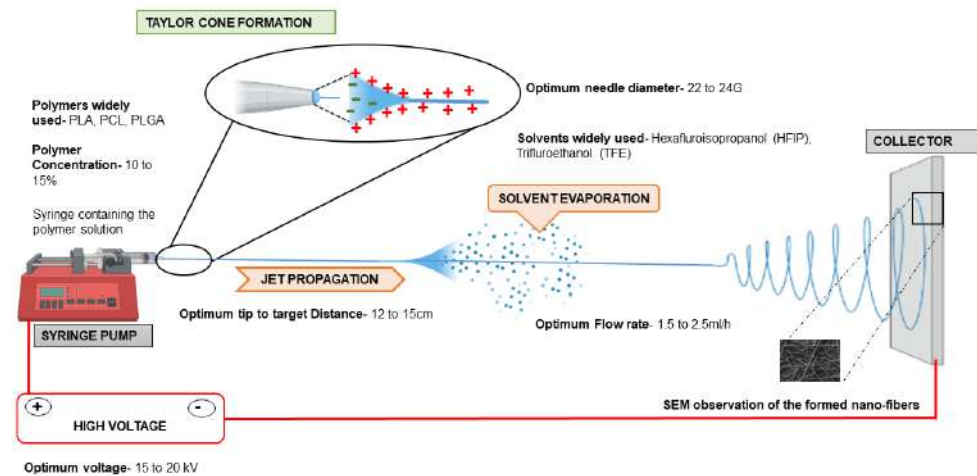


Figure 3. Optimum electrospinning parameters used for liver tissue engineering are provided. Polymers such as PLA, PCL and PLGA are most commonly used at a concentration of 10–15% dissolved in solvents such as HFIP, TFE, etc. The needle used for electrospinning has a diameter of 20–24 G and the tip to target distance should be about 12–15 cm. The voltage of the equipment should be maintained at 15–20 kV. The flow rate of the polymers should be 1.5 to 2.5 mL/h. With these parameters, the obtained fiber diameter and porosity is approximately around 400–450 nm and 40 μ m, respectively, and is suitable for hepatic cells. PLA: Polylactic acid; PCL: Polycaprolactone; PLGA: Polylactic-co-glycolic acid; HFIP: Hexafluoro-isopropanol; TFE: Trifluoroethanol (unpublished original pictures by authors created using Biorender.com). PCL is another widely used polymer for liver tissue engineering applications.

PCL is effective in facilitating cellular growth and proliferation. However, to overcome the hydrophobicity of this polymer and also to improve its mechanical properties, this polymer is also combined with natural polymers and/or tissue matrix proteins. PCL combined with collagen and PES polymer has shown effective hepatic differentiation of the hMSCs [86]. Bishi et al. have shown that a co-polymer of these two polymers, PLA and PCL (PLACL), is most suitable for liver cells due to its highly lipophilic nature [87]. This study has used a blend of PLACL and collagen in the ratio (2:1) along with hMSCs for trans-differentiation into hepatocytes. The addition of collagen to the PLACL polymer resulted in a more hydrophilic polymer suitable for attachment of the hMSCs. The tensile strength was reduced after the collagen blend, yet the elastic modulus remained the same as that of the PLACL alone. The cell number was increased gradually on the PLACL/collagen scaffold starting from day 7 till day 28. The hMSCs' phenotype was maintained till day 7 and, upon treatment with dexamethasone and other liver-specific growth factors, the cells attained polygonal morphology similar to the hepatocytes, which was maintained until day 28 on the PLACL/collagen scaffolds. The differentiation of the hMSCs into hepatocytes was also confirmed with an increased gene expression of hepatocyte nuclear factor 4 alpha (HNF4a) and albumin and a decreased expression of alpha-fetoprotein (AFP) from day 14 to 28. Albumin secretion was also enhanced in the hepatospheres grown on the PLACL/collagen scaffold at day 28. The extent of differentiation from hMSCs to hepatocytes was not very significant in scaffolds with PLACL alone. Hence, we can conclude that, although synthetic polymers are capable of supporting the culture of hepatic cells, the inclusion of a suitable biological component facilitates better attachment, adhesion and prolonged functional features of the cells on these scaffolds.

5. Electrospun Natural Polymers for Liver Cell Cultures

Natural polymers are also used in tissue engineering, but not as widely as synthetic ones, due to their compromised mechanical strength and problems in tunability according to the user's experiment. Chitosan is one of the suitable natural polymers for hepatocytes, because it is structurally similar to the glycosaminoglycans present in the liver ECM. A wide variety of matrix proteins such as collagen, fibronectin, epibolin and chondronectins are used as coating for culturing hepatocytes *in vitro*, with collagen being the most widely used protein. However, collagen or fibronectin alone cannot be used as an electrospun scaffold, due to their poor mechanical strength. A study has reported the use fibronectin along with electrospun chitosan scaffolds [69]. Primary hepatocytes cultured on these fibronectin-coated chitosan films exhibited their characteristic polygonal morphology, whereas the cells cultured on 2D chitosan films alone maintained a round morphology. The same pattern was also observed between fibronectin-coated electrospun chitosan nanofibers and electrospun chitosan nanofibers alone. Cell viability confirmed with calcein-AM staining was markedly improved with fibronectin coating on electrospun chitosan nanofibers. Hepatocytes have a distinct feature of robust communication with their neighboring cells such as Kupffer cells, sinusoidal endothelial cells and fibroblasts. Their morphology and functions largely depend on their cross talk with these neighboring cells. In this study, the authors illustrated that the hepatocytes co-cultured with the fibroblasts on layers of chitosan fibers coated with fibronectin in a 3D environment maintained their morphology and enhanced albumin secretion for about 18 days in comparison to monoculture of the hepatocytes. The cell migration and adhesion were higher on the electrospun scaffolds than on the films, showing the efficiency of the porous nature of the nanofibrous scaffolds developed by the electrospinning technique. The P450 functional activity of the seeded cells was also increased with the 3D co-culture system of electrospun scaffolds, when compared to monoculture systems. P450 activity of hepatocytes is a crucial functional property of the cells to be considered, when the cells on scaffolds are meant to serve as a device for drug testing.

With evolving trends in electrospinning, natural polymers are now being blended with synthetic components to create scaffolds that can support cells *in vitro* as well as *in vivo*. Silk fibroin is one such biopolymer that has been widely explored by scientists for tissue engineering applications given its resemblance with collagen [66]. Electrospinning silk fibroin, however, often shows bead formation along with the nanofibers formed. To overcome this difficulty, PEO (Polyethylene Oxide) synthetic polymer has been incorporated along with silk fibroin and galactosylated chitosan for obtaining linear fibers without the beads. The advantage of using natural polymer is that, due to its hydrophilicity, it can retain water more than the synthetic scaffolds without much swelling [88]. Kasoju et al. have shown that the swelling degree of the silk-fibroin-based galactosylated polymer was only 2%, whereas its water retention capacity was 75%. HepG2 cells cultured on these modified silk-based scaffolds for a period of 7 days showed an increase in cell density with time. It was also observed that the cells attained a spheroid morphology with the help of galactosylated surface modifications on the scaffolds. Several other studies [79–81] have also reported that galactosylated surfaces can induce the spheroid formation of the cells on the natural polymers. Bishi et al. reported that human BMSCs successfully trans-differentiated toward functional hepatocytes on the nanofibrous scaffolds, which were formed by the combination of a natural polymer, gelatin and a synthetic polymer, PLLA [81]. The nanofibrous scaffolds supported cell adhesion, proliferation and efficient commitment of hBMSCs towards metabolically competent hepatocytes (with enhanced albumin secretion and CYP3A4 activity). The topography of PLLA/gelatin nanofibers guided cell morphogenesis through enhanced integrin attachment during hepatic differentiation of hBMSCs (Figure 4). This approach of using modified electrospun scaffolds thus holds great promise for creating disease-specific, *ex vivo* engineered liver tissues for clinical translation studies.

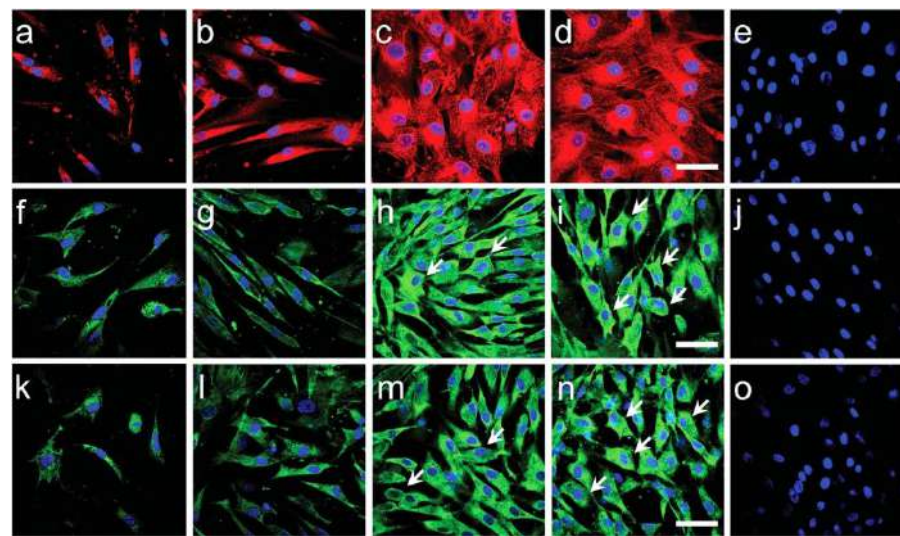


Figure 4. Reprinted with permission. Bishi DK et al., *Adv Healthc Mater.* 2016; 1058-70. Hepatocyte-specific marker expression (α -fetoprotein, albumin and cytokeratin-18) in BMSCs-derived hepatocyte-like cells as shown by confocal microscopy images (merged) on (a,f,k) PLLA scaffold with recombinant hepatic growth factor induction, (b,g,l) PLLA scaffold with hepatogenic serum induction, (c,h,m) PLLA/gelatin with recombinant hepatic growth factor induction, (d,i,n) PLLA/gelatin scaffold with hepatogenic serum induction at day 28. Alexa Fluor-594 labelled α -fetoprotein (a–d: red), Alexa Fluor-488 labelled albumin (f–i: green) and Alexa Fluor-488 labelled cytokeratin-18 (k–n: green) expression represents features of hepatocyte-like cells. (e,j,o) Undifferentiated BMSCs on PLLA/gelatin scaffolds did not express any hepatic markers. Nuclei were stained with DAPI (blue). Compared to PLLA scaffolds, more mature hepatocyte-like cells with cuboidal-to-polygonal morphology were observed (shown by white arrows) on PLLA/gelatin scaffolds in either induction condition (scale bar = 100 μ m.) [81].

6. Liver Extracellular Matrix-Based Electrospun Scaffolds

Several studies are now focusing on incorporating the liver ECM as a whole or in part in the electrospun fibrous scaffolds for providing the growing hepatocytes with the native microenvironment. ECM is crucial for a cell to maintain its phenotype and any changes in its components can drastically change the morphology of a cell. In tumors, cells attaining migratory potential (transformation from epithelial to mesenchymal phenotype) and angiogenic properties are widely dependent on the changes in the ECM of tumor cells. Liver ECM is mainly composed of type I, II, IV and type IX collagen. Other than this, glycoproteins, such as laminin, fibronectin, tenascin and nidogen, and the normal proteoglycans heparin sulphate and chondroitin sulphate are also present in the ECM [89,90]. ECM-modified scaffolds can also be infused with hepatocyte-specific growth factors to achieve maximum functionality. Slivac et al. compared the viability of HepG2 cells when cultured on decellularized liver ECM scaffolds and on PCL mats. It was observed that the cell viability was greatly improved on the ECM scaffolds than on the PCL scaffolds [91]. Grant et al. used decellularized human liver ECM and mixed it with the polymer solution to make blended electrospun scaffolds for THLE-3 liver cell lines. PLLA was used as the polymer in this study and the decellularized liver powder was mixed with 0.25 M acetic acid and then mixed with the polymer solution in the ratio of 1:9 and the electrospinning was performed at a 2.5 mL/h flow rate. The Young's modulus of the scaffold revealed that the blended scaffold with the ECM was stiffer than the conventional polymer scaffold without the decellularized Liver ECM (dLEM). They observed better cell viability with the cells cultured on the dLEM scaffold in comparison with scaffold without dLEM at day 5. An increased albumin secretion by the hepatic cells cultured on the scaffold with dLEM was reported, while the scaffolds modified with the individual ECM components (collagen, fibronectin and laminin) did not show such improvements, indicating improved functionality of the hepatocytes when grown on whole liver matrix [92]. Earlier, this

group also reported a novel method to produce dLEM-based scaffolds for cultures [93]. Here, electrospun PLA scaffolds were used, on which an initial layer of epithelial cells was cultured and transfected with human fibronectin vector. Later, the seeded epithelial layer of cells was decellularized with detergents such that the ECM components were intact on the PLA discs and then further HepG2 cells were grown on the decellularized PLA discs. Although the study put forward a novel approach of cell-derived ECM for hepatic cell cultures, the major limitation of this study is that remnant detergents on the scaffolds after the decellularization process might affect the viability of cultured hepatic cells and there is also a possibility that the scaffolds might be partially degraded if electrospinning had not been performed with care, and also if the concentration of the detergents was not optimized. Besides hepatic cell lines, researchers have also used primary hepatocytes on ECM-based electrospun scaffolds. Most of the studies have shown to preserve hepatocytes in their original morphology for up to 7 days on these scaffolds. Brown et al. reported improved functions of primary human hepatocytes cultured on ECM-modified electrospun scaffolds, highlighting the role of matrix proteins in affecting primary hepatocyte morphology and function. This study used the wet electrospinning technique to obtain nanofibers with increased pore sizes. By this method, the fibers were collected in a liquid bath to avoid a dense accumulation of the fibers and increased pore size. The polymer used in this study was PLGA, which was surface-modified by EDC/NHS (N-(3-Dimethylaminopropyl)-N'-ethyl carbodiimide hydrochloride and N-hydroxysuccinimide) to allow increased attachment of the matrix proteins later attached on the scaffolds. The authors used both collagen and fibronectin in a ratio of 2:1 to mimic the composition of native liver matrix, which contains 60% collagen and 30% non-collagenous proteins. An average pore size of 30 μm was obtained by the wet electrospinning technique, which is the actual average pore size of a human liver tissue, while the pore size obtained by the conventional spinning technique was only 10 μm . Cross-sectional analysis of SEM revealed higher infiltration of the hepatocytes in the scaffolds prepared by wet electrospinning than those prepared by the conventional technique. Hepatocytes on the surface of scaffolds modified with matrix proteins showed better attachment, spreading and morphology when compared to the unmodified scaffolds. Expression of the albumin gene was 3.5-fold higher on collagen-modified scaffolds when compared to the unmodified scaffolds. The CYP3A4 activity of the hepatocytes cultured on the collagen-modified scaffolds was also increased by about fourfold. The albumin and urea secretion increased ten times from day 2 to day 14 on the collagen-modified scaffolds in comparison to the unmodified scaffolds. The study thus concluded that collagen-modified scaffolds are better than unmodified or fibronectin-modified scaffolds [94]. Bual et al. assessed the functions of primary rat hepatocytes cultured on PCL/gelatin electrospun scaffolds incorporated with decellularized porcine liver ECM. Tissue-like aggregation of the cultured hepatocytes was seen on the scaffolds with the highest amount of ECM incorporation at day 7. This was supported by increased albumin secretion and CYP enzyme activity on the same day [95]. Thus, incorporation of decellularized liver ECM blended with natural/synthetic polymers may serve as one of the most effective nanofiber scaffolds for maintaining the viability and functionality of primary hepatocytes. Table 1 summarizes different studies that has used electrospinning for liver tissue engineering.

Table 1. Summary of the different polymers and their electrospinning strategies used in liver tissue engineering to date.

Type of Polymer	Polymer	Cell Type	Modification	Electrospinning Method	Major Observations	Reference
I. Natural	Chitosan	Hepa 1–6	Chitosan + PCL	Conventional electrospinning	Improved cell viability	[58]
		Primary rat hepatocytes	Surface modified with galactose	Conventional electrospinning	Improved functional activity of hepatocytes (increased Albumin, Urea secretion and improved P450 activity) on the galactosylated chitosan nanofibers	[61]
		Primary rat hepatocytes	—	Conventional electrospinning	Albumin production increased 1.5 to 2 fold on the nanofiber scaffolds	[65]
		Primary rat hepatocytes	Fibronectin coating	Conventional electrospinning	CYP activity increased	[69]
	SILK	—	PEO + silk	Conventional electrospinning	Bead less Fiber formation of silk fibroin	[88]
II. Synthetic	PLA	HepG2	Lecithin incorporation	Conventional electrospinning	Increased cell proliferation	[67]
		—	PLA + PCL	Melt electrospinning	Fibers deposited onto pork liver for wound dressing applications	[45]
	PCL	HepG2	—	Conventional electrospinning	Comparison of cell viability on PCL mats and ECM tissue	[91]
		HepG2	Galactosylation and Chitosan incorporation	Conventional electrospinning	Improved cell growth and proliferation	[77]
		HepG2 And primary mouse hepatocytes	—	Conventional electrospinning	Increased Proliferation observed with changed fiber orientation whereas functions like albumin and CYP activity remained the same	[49]
		Human primary hepatocytes HUVECs	3D Printed and stacked	Melt electrospinning	Transplanted scaffolds improved survival and reversal of acute injury	[96]
		Primary rat hepatocytes	Gelatin and ECM incorporation	Conventional electrospinning	Increased albumin secretion	[95]

Table 1. Cont.

Type of Polymer	Polymer	Cell Type	Modification	Electrospinning Method	Major Observations	Reference
PLLA		hMSCs	Gelatin incorporated	Conventional electrospinning	Increased albumin secretion and CYP3A4 activity	[81]
		HMSCs	Plasma treatment and collagen incorporation	Conventional electrospinning	Trans differentiation of MSCs into hepatocytes and increased albumin secretion up to 21 days	[82]
		Primary rat hepatocytes	NH3 Plasma treatment and Type I collagen incorporation	Conventional electrospinning	Hepatocyte aggregation observed, along with increased albumin urea secretion and CYP1A enzyme activity	[64]
		HepG2	Epithelial cell layer seeded and decellularized to obtain matrix incorporated scaffolds	Conventional electrospinning	Increased albumin, CYP and COLA1 gene expression on ECM decorated scaffolds	[93]
		THLE3	Decellularized human tissue ECM incorporated	Conventional electrospinning	Increased attachment and survival of cells, along with increased albumin secretion	[92]
PLGA		Huh7.5	Collagen and fibronectin incorporated at different ratios	Wet electrospinning method	Viability, albumin secretion and CYP gene activity improved	[46]
		Primary human hepatocytes	Collagen and fibronectin incorporated at ratios mimicking matrix composition	Wet electrospinning method	3.5 fold increase in albumin gene expression and 4 fold increase in CYP Gene expression with the protein loaded scaffolds	[94]
PCLEEP		Primary rat hepatocytes	Galactosylated surface	Conventional Electrospinning	Improved albumin secretion and P450 activity	[75]
		Primary rat hepatocytes	3-MC inducer of P450 loaded scaffolds	Conventional Electrospinning	1.5 fold increase in P450 activity	[80]
PLACL		hMSCs	Collagen incorporation	Conventional Electrospinning	Increased expression of HNF4A and albumin	[87]

7. Recent Innovative Approaches in Electrospinning for Liver Tissue Engineering

For prolonged cultures of hepatocytes, studies have now reported the use of hepatic cells in the form of 3D spheroids. Innovative approaches have been employed by researchers to incorporate the hepatocytes as spheroids, which is discussed in the following section. Wei et al. modified the conventional electrospinning method and came up with the idea of short fibers to support culture of hepatic spheroids without the need for surface modifications. They reported that the length of the fibers can be modified according to the length of the spheroids and showed that spheroids cultured on the PSMA (Poly(styrene-co-methyl acrylate) fibers of about 50 μm length have improved drug metabolism and drug clearance [97]. Carbon nanotubes (CNTs) in the form of nanofibrous mats are known to provide electrically conductive surfaces and have been used for prolonged 3D spheroid cultures [98]. Koga et al. have reported that CNTs have the ability to induce the formation of hepatocyte spheroids [99]. Wei et al. have also used multiwalled CNTs functionalized with galactose moieties on the surface for efficient hepatic spheroid cultures. They demonstrated that hepatocytes cultured on these functionalized fibrous mats showed better functions, namely, better drug clearance and increased expression of drug metabolizing genes [100].

Besides in vitro cultures, electrospun liver scaffolds are also being used for in vivo applications. The scaffolds can be fabricated as patches containing nano-fibrous mesh that can then be implanted at the site of injury. Kim et al. have recently shown that electrospun scaffold patches can be used to deliver healthy hepatic cells in toxin-induced liver injury mouse models. In this study, they used PCL for fabricating electrospun scaffolds/sheets and seeded them with patient-derived primary hepatocytes in a stacking manner by 3D bioprinting to mimic the native liver environment. The survival of the animals with the hepatic sheet transplant was 70% as compared to that of the control group without the scaffold. This study has opened the doors of using electrospun liver cell scaffolds for liver transplantation and in vivo therapy [96]. Another study by Salerno et al. has also proved the potential of electrospinning in mimicking the native liver tissue architecture with multiple cell types. They used the dry jet–wet electrospinning method to prepare hollow PCL fibers, and placed them in a bioreactor which contained an outer luminal segment where primary human hepatocytes were cultured and an inner luminal segment where endothelial cells were seeded in a hexagonal manner, thereby mimicking the native liver architecture [101]. The authors observed improved hepatic functions such as glucose consumption and albumin secretion for up to 18 days in the perfusion bioreactor. The recent studies on the electrospun scaffolds show the potential of them on the clinical front, an overview of the recent strategies employed for the fabrication of electrospun nanofiber scaffolds for liver cells is given schematically in Figure 5. Patient-specific scaffolds made out of this technique would give us the edge of replacing liver transplantation treatment with tissue engineering.

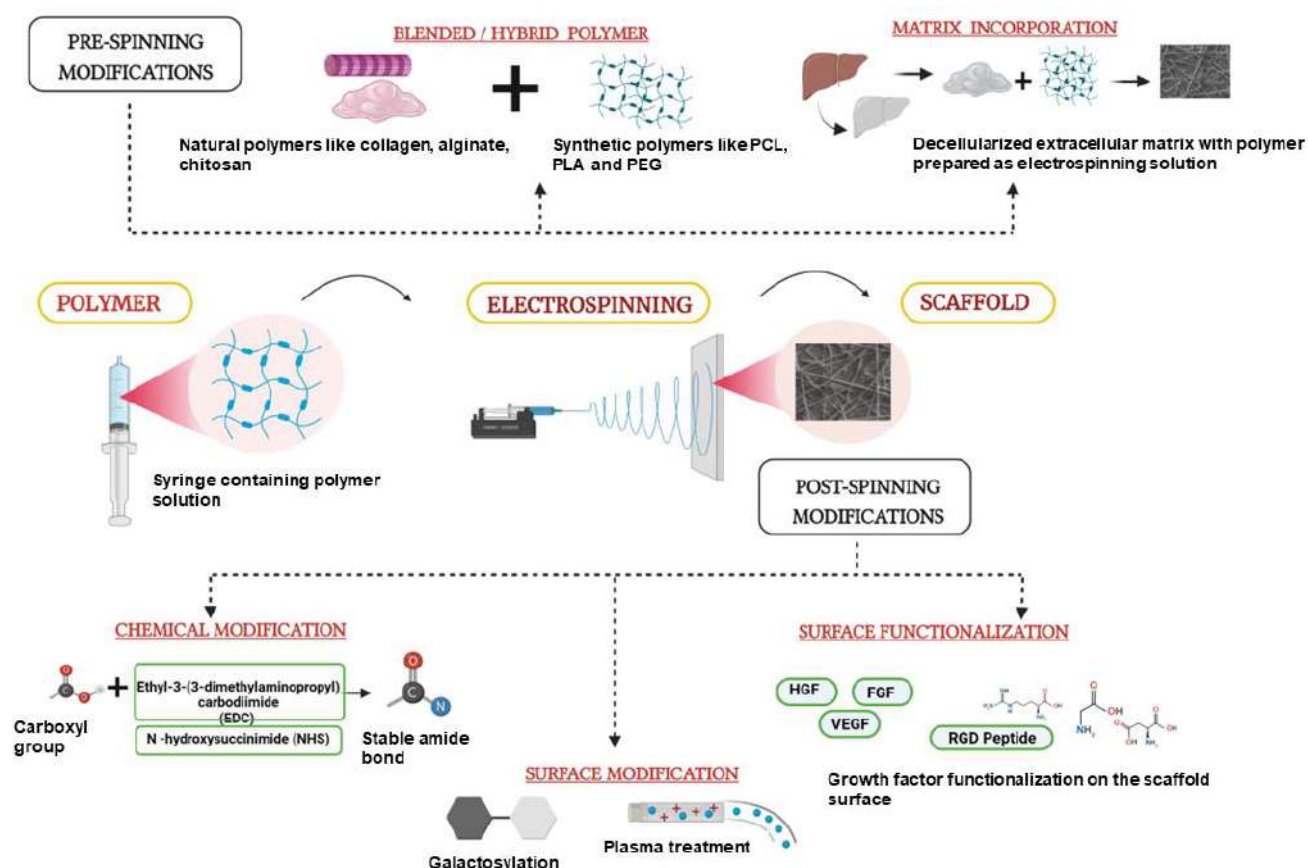


Figure 5. New Strategies employed in Electrospinning for Liver Tissue Engineering. Pre-spinning modifications including incorporation of matrix proteins, drugs or decellularized whole tissue matrix. Post-electrospinning strategies such as surface modification of the fibers with galactose, growth factors and RGD peptide conjugation, thereby improving the quality and functionality of the developed fibers for culture of liver cells. HGF—Hepatocyte Growth Factor, FGF—Fibroblast growth factor, VEGF—Vascular Endothelial Growth Factor (Unpublished original picture by authors created using [Biorender.com](https://www.biorender.com/)).

8. Conclusions

Reproducing the functions of the liver in total or in part for several downstream applications has remained a formidable task. The major hurdle in reproducing liver tissue *ex vivo* is the progressive loss of functions of the hepatocytes within a span of few days under these conditions. Electrospun fibrous scaffolds with a myriad of modifications serve as excellent cell-supporting substrates by providing nanoscale fibrous structures with interconnecting pores, resembling natural tissue ECM. Electrospinning with both natural and synthetic polymers and now also decellularized liver ECM has enormous potential in the development of liver tissue scaffolds with complex geometric/architectural structures. However, we still need many more advancements in the field. Culturing of hepatocytes on electrospun scaffolds as 3D spheroid cultures would lead to better growth and functions of hepatocytes as compared to 2D cultures. Additionally, a co-culture of hepatocytes along with other liver cells such as endothelial and hepatic stellate cells would impart better functionality to the hepatocytes. The success of the cell cultures on the fabricated scaffolds would also largely depend on the topology, composition and mechanical properties of the acellular scaffold. Properties such as optimum matrix stiffness and pore size would be important for achieving appropriate cell–ECM interactions. As our knowledge about the complexities of native liver ECM improves, newer modified biomaterials coupled with improved protocols for electrospinning would allow the fabrication of efficient scaffolds that would facilitate proliferation and differentiation of the primary hepatocytes and

spheroids. Finally, the perfusion of the fabricated cell-seeded electrospun scaffolds under dynamic culture conditions in microfluidic devices would allow fabrication of the most apt working model of the liver sinusoid. Interdisciplinary collaborations would be necessary to undertake these challenges. The day is not far when these steps and developments in the field of electrospinning would allow us to reconstruct an efficient and functional liver tissue that could not only be used in vitro but also for clinical applications in vivo.

Author Contributions: S.K., S.R. and J.R.V. conceptualized the review, A.V. wrote the manuscript, D.M.T. designed the figures, S.S. provided inputs for the write-up, S.K., S.R. and J.R.V. edited the review, S.K. and A.V. finalized the review and all authors approved the manuscript. All authors have read and agreed to the published version of the manuscript.

Funding: The study was funded by the Department of Science and Technology, via ASEAN Grant (CRD/2019/000120).

Institutional Review Board Statement: Not applicable.

Data Availability Statement: Not applicable.

Conflicts of Interest: The authors declare no conflict of interest.

References

1. Anbusagar, N.; Palanikumar, K.; Ponshanmugakumar, A. Preparation and properties of nanopolymer advanced composites: A review. In *Polymer-based Nanocomposites for Energy and Environmental Applications*; Woodhead Publishing: Sawston, UK, 2018; pp. 27–73. ISBN 9780081022627.
2. Chandrasekaran, A.R.; Venugopal, J.; Sundarrajan, S.; Ramakrishna, S. Fabrication of a nanofibrous scaffold with improved bioactivity for culture of human dermal fibroblasts for skin regeneration. *Biomed. Mater.* **2011**, *6*, 015001. [\[CrossRef\]](#)
3. Ravichandran, R.; Venugopal, J.R.; Sundarrajan, S.; Mukherjee, S.; Ramakrishna, S. Precipitation of nanohydroxyapatite on PLLA/PBLG/Collagen nanofibrous structures for the differentiation of Adipose Derived Stem Cells to Osteogenic lineage. *Biomaterials* **2012**, *33*, 846–855. [\[CrossRef\]](#)
4. Sridhar, R.; Venugopal, J.; Sundarrajan, S.; Ravichandran, R.; Ramalingam, B.; Ramakrishna, S. Electrospun nanofibers for pharmaceutical and medical applications. *J. Drug Deliv. Sci. Technol.* **2011**, *21*, 451–468. [\[CrossRef\]](#)
5. Ravichandran, R.; Venugopal, J.R.; Sundarrajan, S.; Mukherjee, S.; Sridhar, R.; Ramakrishna, S. Composite poly-L-lactic acid/poly-(α,β)-DL-aspartic acid/collagen nanofibrous scaffolds for dermal tissue regeneration. *Mater. Sci. Eng. C* **2012**, *32*, 1443–1451. [\[CrossRef\]](#) [\[PubMed\]](#)
6. Badylak, S.F.; Freytes, D.O.; Gilbert, T. Extracellular matrix as a biological scaffold material: Structure and function. *Acta Biomater.* **2009**, *5*, 1–13. [\[CrossRef\]](#)
7. Cavalcanti-Adam, E.A.; Aydin, D.; Hirschfeld-Warneken, V.C.; Spatz, J.P. Cell adhesion and response to synthetic nanopatterned environments by steering receptor clustering and spatial location. *HFSP J.* **2008**, *2*, 276–285. [\[CrossRef\]](#)
8. Pangesty, A.I.; Todo, M. Improvement of mechanical strength of tissue engineering scaffold due to the temperature control of polymer blend solution. *J. Funct. Biomater.* **2021**, *12*, 47. [\[CrossRef\]](#) [\[PubMed\]](#)
9. Radakisnin, R.; Majid, M.S.A.; Jamir, M.R.M.; Tahir, M.F.M.; Meng, C.E.; Al Alshahrani, H. Physical, thermal, and mechanical properties of highly porous polylactic acid/cellulose nanofibre scaffolds prepared by salt leaching technique. *Nanotechnol. Rev.* **2021**, *10*, 1469–1483. [\[CrossRef\]](#)
10. He, B.; Yuan, X.; Jiang, D. Molecular self-assembly guides the fabrication of peptide nanofiber scaffolds for nerve repair. *RSC Adv.* **2014**, *4*, 23610–23621. [\[CrossRef\]](#)
11. Aghajanpoor, M.; Hashemi-Najafabadi, S.; Baghaban-Eslaminejad, M.; Bagheri, F.; Mohammad Mousavi, S.; Azam Sayyapour, F. The effect of increasing the pore size of nanofibrous scaffolds on the osteogenic cell culture using a combination of sacrificial agent electrospinning and ultrasonication. *J. Biomed. Mater. Res. Part A* **2017**, *105*, 1887–1899. [\[CrossRef\]](#)
12. Luketich, S.K.; Cosentino, F.; Di Giuseppe, M.; Menallo, G.; Nasello, G.; Livreri, P.; Wagner, W.R.; D'Amore, A. Engineering in-plane mechanics of electrospun polyurethane scaffolds for cardiovascular tissue applications. *J. Mech. Behav. Biomed. Mater.* **2022**, *128*, 105126. [\[CrossRef\]](#) [\[PubMed\]](#)
13. Kawakami, Y.; Nonaka, K.; Fukase, N.; Amore, A.D.; Murata, Y.; Quinn, P.; Luketich, S.; Takayama, K.; Patel, K.G.; Matsumoto, T.; et al. A cell-free biodegradable synthetic artificial ligament for the reconstruction of anterior cruciate ligament in a rat model. *Acta Biomater.* **2021**, *121*, 275–287. [\[CrossRef\]](#) [\[PubMed\]](#)
14. Ranganathan, S.; Balagangadharan, K.; Selvamurugan, N. Chitosan and gelatin-based electrospun fibers for bone tissue engineering. *Int. J. Biol. Macromol.* **2019**, *133*, 354–364. [\[CrossRef\]](#) [\[PubMed\]](#)
15. Gautam, S.; Sharma, C.; Purohit, S.D.; Singh, H.; Dinda, A.K.; Potdar, P.D.; Chou, C.-F.; Mishra, N.C. Gelatin-polycaprolactone-nanohydroxyapatite electrospun nanocomposite scaffold for bone tissue engineering. *Mater. Sci. Eng. C* **2021**, *119*, 111588. [\[CrossRef\]](#)

16. Lin, W.; Chen, M.; Qu, T.; Li, J.; Man, Y. Three-dimensional electrospun nanofibrous scaffolds for bone tissue engineering. *J. Biomed. Mater. Res. Part B Appl. Biomater.* **2020**, *108*, 1311–1321. [[CrossRef](#)] [[PubMed](#)]
17. Peranidze, K.; Safronova, T.V.; Kildeeva, N.R. Fibrous polymer-based composites obtained by electrospinning for bone tissue engineering. *Polymers* **2021**, *14*, 96. [[CrossRef](#)]
18. Lowery, J.L.; Datta, N.; Rutledge, G.C. Effect of fiber diameter, pore size and seeding method on growth of human dermal fibroblasts in electrospun poly (ϵ -caprolactone) fibrous mats. *Biomaterials* **2010**, *31*, 491–504. [[CrossRef](#)]
19. Asrani, S.K.; Devarbhavi, H.; Eaton, J.; Kamath, P.S. Burden of liver diseases in the world. *J. Hepatol.* **2019**, *70*, 151–171. [[CrossRef](#)] [[PubMed](#)]
20. Verdonk, R.C.; van den Berg, A.P.; Slooff, M.J.; Porte, R.J.; Haagsma, E.B. Liver transplantation: An update. *Neth. J. Med.* **2007**, *65*, 372–380. [[PubMed](#)]
21. Skagen, C.; Lucey, M.A. Liver transplantation: An update. *Curr. Opin. Gastroenterol.* **2009**, *25*, 202–208. [[CrossRef](#)] [[PubMed](#)]
22. Ellis, A.J.; Hughes, R.D.; Wendon, J.A. Pilot-controlled trial of the extracorporeal liver assist device in acute liver failure. *Hepatology* **1996**, *24*, 1446–1451. [[CrossRef](#)] [[PubMed](#)]
23. Sussman, N.L.; Gislason, G.T.; Conlin, C.A.; Kelly, J.H. The Hepatix extracorporeal liver assist device: Initial clinical experience. *Artif. Organs* **1994**, *18*, 390–396. [[CrossRef](#)] [[PubMed](#)]
24. Mitzner, S.R.; Stange, J.; Klammt, S. Extracorporeal detoxification using the molecular adsorbent recirculating system for critically ill patients with liver failure. *J. Am. Soc. Nephrol.* **2001**, *12* (Suppl. S1), S75–S82. [[CrossRef](#)]
25. Agarwal, T.; Subramanian, B.; Maiti, T.K. Liver tissue engineering: Challenges and opportunities. *ACS Biomater. Sci. Eng.* **2019**, *5*, 4167–4182. [[CrossRef](#)] [[PubMed](#)]
26. Kaur, S.; Tripathi, D.M.; Venugopal, J.R.; Ramakrishna, S. Advances in biomaterials for hepatic tissue engineering. *Curr. Opin. Biomed. Eng.* **2020**, *13*, 190–196. [[CrossRef](#)]
27. Tillman, B.W.; Yazdani, S.K.; Lee, S.J.; Geary, R.L.; Atala, A.; Yoo, J.J. The in vivo stability of electrospun polycaprolactone-collagen scaffolds in vascular reconstruction. *Biomaterials* **2009**, *30*, 583–588. [[CrossRef](#)]
28. Kumbar, S.G.; Nukavarapu, S.P.; James, R.; Hogan, M.V.; Laurencin, C.T. Recent patents on electrospun biomedical nanostructures: An overview. *Recent Pat. Biomed. Eng.* **2008**, *1*, 68–78.
29. Shahriar, S.M.; Mondal, J.; Hasan, M.N.; Revuri, V.; Lee, D.Y.; Lee, Y.K. Electrospinning nanofibers for therapeutics delivery. *Nanomaterials* **2019**, *9*, 532. [[CrossRef](#)]
30. Sayin, S.; Tufani, A.; Emanet, M.; Genchi, G.G.; Sen, O.; Shemshad, S.; Ozaydin Ince, G. Electrospun nanofibers with pH-responsive coatings for control of release kinetics. *Front. Bioeng. Biotechnol.* **2019**, *7*, 309. [[CrossRef](#)]
31. Volpato, F.Z.; Almodóvar, J.; Erickson, K.; Popat, K.C.; Migliaresi, C.; Kipper, M.J. Preservation of FGF-2 bioactivity using heparin-based nanoparticles, and their delivery from electrospun chitosan fibers. *Acta Biomater.* **2012**, *8*, 1551–1559.
32. Almodóvar, J.; Kipper, M.J. Coating electrospun chitosan nanofibers with polyelectrolyte multilayers using the polysaccharides heparin and N, N, N-trimethyl chitosan. *Macromol. Biosci.* **2011**, *11*, 72–76. [[CrossRef](#)] [[PubMed](#)]
33. Luong-Van, E.; Grøndahl, L.; Chua, K.N.; Leong, K.W.; Nurcombe, V.; Cool, S.M. Controlled release of heparin from poly (ϵ -caprolactone) electrospun fibers. *Biomaterials* **2006**, *27*, 2042–2050. [[CrossRef](#)] [[PubMed](#)]
34. Karpov, T.E.; Peltek, O.O.; Muslimov, A.R.; Tarakanchikova, Y.V.; Grunina, T.M.; Poponova, M.S.; Surmenev, R.A. Development of optimized strategies for growth factor incorporation onto electrospun fibrous scaffolds to promote prolonged release. *ACS Appl. Mater. Interfaces* **2019**, *12*, 5578–5592. [[CrossRef](#)] [[PubMed](#)]
35. Liu, C.; Wang, C.; Zhao, Q.; Li, X.; Xu, F.; Yao, X.; Wang, M. Incorporation and release of dual growth factors for nerve tissue engineering using nanofibrous bicomponent scaffolds. *Biomed. Mater.* **2018**, *13*, 044107. [[CrossRef](#)] [[PubMed](#)]
36. Sahoo, S.; Ang, L.T.; Goh, J.C.; Toh, S.L. Growth factor delivery through electrospun nanofibers in scaffolds for tissue engineering applications. *J. Biomed. Mater. Res. Part A* **2010**, *93*, 1539–1550. [[CrossRef](#)]
37. Yin, Z.; Chen, X.; Song, H.X.; Hu, J.J.; Tang, Q.M.; Zhu, T.; Shen, W.L.; Chen, J.L.; Liu, H.; Heng, B.C.; et al. Electrospun scaffolds for multiple tissues regeneration in vivo through topography dependent induction of lineage specific differentiation. *Biomaterials* **2015**, *44*, 173–185. [[CrossRef](#)]
38. Blackwood, K.A.; McKean, R.; Canton, I.; Freeman, C.O.; Franklin, K.L.; Cole, D.; MacNeil, S. Development of biodegradable electrospun scaffolds for dermal replacement. *Biomaterials* **2008**, *29*, 3091–3104.
39. Klumpp, D.; Rudisile, M.; Kühnle, R.I.; Hess, A.; Bitto, F.F.; Arkudas, A.; Bleiziffer, O.; Boos, A.M.; Kneser, U.; Horch, R.E.; et al. Three-dimensional vascularization of electrospun PCL/collagen- blend nanofibrous scaffolds in vivo. *J. Biomed. Mater. Res. Part A* **2012**, *100A*, 2302–2311. [[CrossRef](#)]
40. Yu, D.G.; Chian, W.; Wang, X.; Li, X.Y.; Li, Y.; Liao, Y.Z. Linear drug release membrane prepared by a modified coaxial electrospinning process. *J. Membr. Sci.* **2013**, *428*, 150–156. [[CrossRef](#)]
41. Yang, J.M.; Zha, L.S.; Yu, D.G.; Liu, J. Coaxial electrospinning with acetic acid for preparing ferulic acid/zein composite fibers with improved drug release profiles. *Colloids Surf. B Biointerfaces* **2013**, *102*, 737–743. [[CrossRef](#)]
42. Place, L.W.; Sekyi, M.; Taussig, J.; Kipper, M.J. Two-Phase Electrospinning to Incorporate Polyelectrolyte Complexes and Growth Factors into Electrospun Chitosan Nanofibers. *Macromol. Biosci.* **2016**, *16*, 371–380. [[CrossRef](#)] [[PubMed](#)]
43. Wang, C.; Hou, W.; Guo, X.; Li, J.; Hu, T.; Qiu, M.; Liu, X. Two-phase electrospinning to incorporate growth factors loaded chitosan nanoparticles into electrospun fibrous scaffolds for bioactivity retention and cartilage regeneration. *Mater. Sci. Eng. C* **2017**, *79*, 507–515. [[CrossRef](#)] [[PubMed](#)]

44. Zhang, L.H.; Duan, X.P.; Yan, X.; Yu, M.; Ning, X.; Zhao, Y.; Long, Y.Z. Recent advances in melt electrospinning. *RSC Adv.* **2016**, *6*, 53400–53414. [[CrossRef](#)]
45. Qin, C.C.; Duan, X.P.; Wang, L.; Zhang, L.H.; Yu, M.; Dong, R.H.; Long, Y.Z. Melt electrospinning of poly (lactic acid) and polycaprolactone microfibers by using a hand-operated Wimshurst generator. *Nanoscale* **2015**, *7*, 16611–16615. [[CrossRef](#)]
46. Das, P.; DiVito, M.D.; Wertheim, J.A.; Tan, L.P. Collagen-I and fibronectin modified three-dimensional electrospun PLGA scaffolds for long-term in vitro maintenance of functional hepatocytes. *Mater. Sci. Eng. C* **2020**, *111*, 110723. [[CrossRef](#)]
47. Ding, Y.; Xu, W.; Xu, T.; Zhu, Z.; Fong, H. Theories and principles behind electrospinning. In *Advanced Nanofibrous Materials Manufacture Technology Based on Electrospinning*; CRC Press: Boca Raton, FL, USA, 2019; pp. 22–51.
48. Al-Dhahebi, A.M.; Ling, J.; Krishnan, S.G.; Yousefzadeh, M.; Elumalai, N.K.; Saheed, M.S.; Ramakrishna, S.; Jose, R. Electrospinning research and products: The road and the way forward. *Appl. Phys. Rev.* **2022**, *9*, 011319. [[CrossRef](#)]
49. Bate, T.S.; Gadd, V.L.; Forbes, S.J.; Callanan, A. Response differences of HepG2 and Primary Mouse Hepatocytes to morphological changes in electrospun PCL scaffolds. *Sci. Rep.* **2021**, *11*, 3059. [[CrossRef](#)]
50. Liu, X.; Ma, P.X. Polymeric scaffolds for bone tissue engineering. *Ann. Biomed. Eng.* **2004**, *32*, 477. [[CrossRef](#)]
51. Kang, B.J.; Kim, H.; Lee, S.K.; Kim, J.; Shen, Y.; Jung, S.; Cho, J.Y. Umbilical-cord-blood-derived mesenchymal stem cells seeded onto fibronectin-immobilized polycaprolactone nanofiber improve cardiac function. *Acta Biomater.* **2014**, *10*, 3007–3017. [[CrossRef](#)]
52. Jiang, X.; Cao, H.Q.; Shi, L.Y.; Ng, S.Y.; Stanton, L.W.; Chew, S.Y. Nanofiber topography and sustained biochemical signaling enhance human mesenchymal stem cell neural commitment. *Acta Biomater.* **2012**, *8*, 1290–1302. [[CrossRef](#)]
53. Nguyen, L.T.; Liao, S.; Ramakrishna, S.; Chan, C.K. The role of nanofibrous structure in osteogenic differentiation of human mesenchymal stem cells with serial passage. *Nanomedicine* **2011**, *6*, 961–974. [[CrossRef](#)] [[PubMed](#)]
54. Pham, Q.P.; Sharma, U.; Mikos, A.G. Electrospinning of polymeric nanofibers for tissue engineering applications: A review. *Tissue Eng.* **2006**, *12*, 1197–1211. [[CrossRef](#)] [[PubMed](#)]
55. Garg, K.; Bowlin, G.L. Electrospinning jets and nanofibrous structures. *Biomicrofluidics* **2011**, *5*, 013403. [[CrossRef](#)]
56. Rahmati, M.; Mills, D.K.; Urbanska, A.M.; Saeb, M.R.; Venugopal, J.R.; Ramakrishna, S.; Mozafari, M. Electrospinning for tissue engineering applications. *Prog. Mater. Sci.* **2020**, *117*, 100721. [[CrossRef](#)]
57. Sukanya, V.S.; Mohanan, P.V. Degradation of Poly (ϵ -caprolactone) and bio-interactions with mouse bone marrow mesenchymal stem cells. *Colloids Surf. B Biointerfaces* **2018**, *163*, 107–118.
58. Semnani, D.; Naghashzargar, E.; Hadjianfar, M.; Dehghan Manshadi, F.; Mohammadi, S.; Karbasi, S.; Effaty, F. Evaluation of PCL/chitosan electrospun nanofibers for liver tissue engineering. *Int. J. Polym. Mater. Polym. Biomater.* **2017**, *66*, 149–157. [[CrossRef](#)]
59. Wang, Y.K.; Yong, T.; Ramakrishna, S. Nanofibres and their influence on cells for tissue regeneration. *Aust. J. Chem.* **2005**, *58*, 704–712. [[CrossRef](#)]
60. Gluck, J.M. Electrospun Poly (E-Caprolactone) (PCL) Nanofibrous Scaffolds for Liver Tissue Engineering. Master's Thesis, North Carolina State University, Raleigh, NC, USA, 18 July 2007.
61. Feng, Z.Q.; Chu, X.; Huang, N.P.; Wang, T.; Wang, Y.; Shi, X.; Gu, Z.Z. The effect of nanofibrous galactosylated chitosan scaffolds on the formation of rat primary hepatocyte aggregates and the maintenance of liver function. *Biomaterials* **2009**, *30*, 2753–2763. [[CrossRef](#)]
62. Matthews, J.A.; Wnek, G.E.; Simpson, D.G.; Bowlin, G.L. Electrospinning of Collagen Nanofibers. *Biomacromolecules* **2002**, *3*, 232–238. [[CrossRef](#)]
63. Ishibashi, H.; Nakamura, M.; Komori, A.; Migita, K.; Shimoda, S. Liver architecture, cell function, and disease. *Semin. Immunopathol.* **2009**, *31*, 399–409. [[CrossRef](#)]
64. Feng, Z.-Q.; Chu, X.-H.; Huang, N.-P.; Leach, M.K.; Wang, G.; Wang, Y.-C.; Ding, Y.-T.; Gu, Z.-Z. Rat hepatocyte aggregate formation on discrete aligned nanofibers of type-I collagen-coated poly (L-lactic acid). *Biomaterials* **2010**, *31*, 3604–3612. [[CrossRef](#)] [[PubMed](#)]
65. Chu, X.-H.; Shi, X.-L.; Feng, Z.-Q.; Gu, Z.-Z.; Ding, Y.-T. Chitosan nanofiber scaffold enhances hepatocyte adhesion and function. *Biotechnol. Lett.* **2009**, *31*, 347–352. [[CrossRef](#)] [[PubMed](#)]
66. Kasoju, N.; Bora, U. Silk fibroin in tissue engineering. *Adv. Healthc. Mater.* **2012**, *1*, 393–412. [[CrossRef](#)]
67. Liu, X.; Zhou, L.; Heng, P.; Xiao, J.; Lv, J.; Zhang, Q.; Wang, J. Lecithin doped electrospun poly (lactic acid)-thermoplastic polyurethane fibers for hepatocyte viability improvement. *Colloids Surf. B Biointerfaces* **2019**, *175*, 264–271. [[CrossRef](#)]
68. Silnutzer, J.E.; Barnes, D.W. Effects of fibronectin-related peptides on cell spreading. *Vitr. Cell. Dev. Biol.* **1995**, *21*, 73–78. [[CrossRef](#)]
69. Rajendran, D.; Hussain, A.; Yip, D.; Parekh, A.; Shrirao, A.; Cho, C.H. Long-term liver-specific functions of hepatocytes in electrospun chitosan nanofiber scaffolds coated with fibronectin. *J. Biomed. Mater. Res. Part A* **2017**, *105*, 2119–2128. [[CrossRef](#)]
70. Bell, C.C.; Dankers, A.C.A.; Lauschte, V.M.; Sison-Young, R.; Jenkins, R.; Rowe, C.; Goldring, C.E.; Park, K.; Regan, S.L.; Walker, T.; et al. Comparison of Hepatic 2D Sandwich Cultures and 3D Spheroids for Long-term Toxicity Applications: A Multicenter Study. *Toxicol. Sci.* **2018**, *162*, 655–666. [[CrossRef](#)] [[PubMed](#)]
71. Chua, K.-N. Surface-aminated electrospun nanofibers enhance adhesion and expansion of human umbilical cord blood hematopoietic stem/progenitor cells. *Biomaterials* **2006**, *27*, 6043–6051. [[CrossRef](#)]
72. Hamilton, G.A.; Jolley, S.L.; Gilbert, D.; Coon, D.J.; Barros, S.; LeCluyse, E.L. Regulation of cell morphology and cytochrome P450 expression in human hepatocytes by extracellular matrix and cell–cell interactions. *Cell Tissue Res.* **2001**, *306*, 85–99. [[PubMed](#)]

73. Richert, L.; Binda, D.; Hamilton, G.; Viollon-Abadie, C.; Alexandre, E.; Bigot-Lasserre, D.; Bars, R.; Coassolo, P.; LeCluyse, E. Evaluation of the effect of culture configuration on morphology, survival time, antioxidant status and metabolic capacities of cultured rat hepatocytes. *Toxicol. Vitro* **2002**, *16*, 89–99. [\[CrossRef\]](#)
74. Lu, H.F.; Chua, K.N.; Zhang, P.C.; Lim, W.S.; Ramakrishna, S.; Leong, K.W.; Mao, H.Q. Three-dimensional co-culture of rat hepatocyte spheroids and NIH/3T3 fibroblasts enhances hepatocyte functional maintenance. *Acta Biomater.* **2005**, *1*, 399–410. [\[CrossRef\]](#) [\[PubMed\]](#)
75. Chua, K.N.; Lim, W.S.; Zhang, P.; Lu, H.; Wen, J.; Ramakrishna, S.; Mao, H.Q. Stable immobilization of rat hepatocyte spheroids on galactosylated nanofiber scaffold. *Biomaterials* **2005**, *26*, 2537–2547. [\[CrossRef\]](#)
76. Chien, H.W.; Lai, J.Y.; Tsai, W.B. Galactosylated electrospun membranes for hepatocyte sandwich culture. *Colloids Surf. B Biointerfaces* **2014**, *116*, 576–581. [\[CrossRef\]](#)
77. Ghahremanzadeh, F.; Alihosseini, F.; Semnani, D. Investigation and comparison of new galactosylation methods on PCL/chitosan scaffolds for enhanced liver tissue engineering. *Int. J. Biol. Macromol.* **2021**, *174*, 278–288. [\[CrossRef\]](#) [\[PubMed\]](#)
78. Liang, D.; Hsiao, B.S.; Chu, B. Functional electrospun nanofibrous scaffolds for biomedical applications. *Adv. Drug Deliv. Rev.* **2007**, *59*, 1392–1412. [\[CrossRef\]](#) [\[PubMed\]](#)
79. Fan, J.; Shang, Y.; Yuan, Y.; Yang, J. Preparation and characterization of chitosan/galactosylated hyaluronic acid scaffolds for primary hepatocytes culture. *J. Mater. Sci. Mater. Med.* **2010**, *21*, 319–327. [\[CrossRef\]](#)
80. Chua, K.N.; Tang, Y.N.; Quek, C.H.; Ramakrishna, S.; Leong, K.W.; Mao, H.Q. A dual-functional fibrous scaffold enhances P450 activity of cultured primary rat hepatocytes. *Acta Biomater.* **2007**, *3*, 643–650. [\[CrossRef\]](#)
81. Bishi, D.K.; Mathapati, S.; Venugopal, J.R.; Guhathakurta, S.; Cherian, K.M.; Verma, R.S.; Ramakrishna, S.A. Patient-Inspired Ex Vivo Liver Tissue Engineering Approach with Autologous Mesenchymal Stem Cells and Hepatogenic Serum. *Adv Healthc. Mater.* **2016**, *5*, 1058–1070. [\[CrossRef\]](#) [\[PubMed\]](#)
82. Liu, S.; Qin, S.; He, M.; Zhou, D.; Qin, Q.; Wang, H. Current applications of poly (lactic acid) composites in tissue engineering and drug delivery. *Compos. Part B Eng.* **2020**, *199*, 108238. [\[CrossRef\]](#)
83. Lv, Q.; Hu, K.; Feng, Q.; Cui, F.; Cao, C. Preparation and characterization of PLA/fibroin composite and culture of HepG2 (human hepatocellular liver carcinoma cell line) cells. *Compos. Sci. Technol.* **2007**, *67*, 3023–3030. [\[CrossRef\]](#)
84. Ghaedi, M.; Soleimani, M.; Shabani, I.; Duan, Y.; Lotfi, A. Hepatic differentiation from human mesenchymal stem cells on a novel nanofiber scaffold. *Cell. Mol. Biol. Lett.* **2012**, *17*, 89–106. [\[CrossRef\]](#)
85. Kazemnejad, S.; Allameh, A.; Soleimani, M.; Gharehbaghian, A.; Mohammadi, Y.; Amirzadeh, N.; Jazayeri, M. Biochemical and molecular characterization of hepatocyte-like cells derived from human bone marrow mesenchymal stem cells on a novel three-dimensional biocompatible nanofibrous scaffold. *J. Gastroenterol. Hepatol.* **2009**, *24*, 278–287. [\[CrossRef\]](#)
86. Kazemnejad, S.; Allameh, A.; Soleimani, M.; Gharehbaghian, A.; Mohammadi, Y.; Amirzadeh, N.; Esmaeili, S. Functional hepatocyte-like cells derived from human bone marrow mesenchymal stem cells on a novel 3-dimensional biocompatible nanofibrous scaffold. *Int. J. Artif. Organs* **2008**, *31*, 500–507. [\[CrossRef\]](#)
87. Bishi, D.K.; Mathapati, S.; Venugopal, J.R.; Guhathakurta, S.; Cherian, K.M.; Ramakrishna, S.; Verma, R.S. Trans- differentiation of human mesenchymal stem cells generates functional hepatospheres on poly (L-lactic acid)-co-poly (ϵ - caprolactone)/collagen nanofibrous scaffolds. *J. Mater. Chem. B* **2013**, *1*, 3972–3984. [\[CrossRef\]](#) [\[PubMed\]](#)
88. Jin, H.J.; Fridrikh, S.V.; Rutledge, G.C.; Kaplan, D.L. Electrospinning Bombyx mori silk with poly(ethyleneoxide). *Biomacromolecules* **2002**, *3*, 1233–1239. [\[CrossRef\]](#)
89. Bedossa, P.; Paradis, V. Liver extracellular matrix in health and disease. *J. Pathol.* **2003**, *200*, 504–515. [\[CrossRef\]](#)
90. Martinez-Hernandez, A.; Amenta, P.S. The hepatic extracellular matrix. *Virchows Arch. A Pathol. Anat. Histopathol.* **1993**, *423*, 77–84. [\[CrossRef\]](#) [\[PubMed\]](#)
91. Livac, I.; Zdraveva, E.; Ivančić, F.; Žunar, B.; Holjevac Grgurić, T.; Gaurina Srček, V.; Svetec, I.K.; Dolenec, T.; Bajsić, E.G.; Tominac Trcin, M.; et al. Bioactivity Comparison of Electrospun PCL Mats and Liver Extracellular Matrix as Scaffolds for HepG2 Cells. *Polymers* **2021**, *13*, 279.
92. Grant, R.; Hallett, J.; Forbes, S.; Hay, D.; Callanan, A. Blended electrospinning with human liver extracellular matrix for engineering new hepatic microenvironments. *Sci. Rep.* **2019**, *9*, 6293.
93. Grant, R.; Hay, D.; Callanan, A. From scaffold to structure: The synthetic production of cell derived extracellular matrix for liver tissue engineering. *Biomed. Phys. Eng. Express* **2018**, *4*, 065015. [\[CrossRef\]](#)
94. Brown, J.H.; Das, P.; DiVito, M.D.; Ivancic, D.; Tan, L.P.; Wertheim, J.A. Nanofibrous PLGA electrospun scaffolds modified with type I collagen influence hepatocyte function and support viability in vitro. *Acta Biomater.* **2018**, *73*, 217–227. [\[CrossRef\]](#)
95. Bual, R.; Kimura, H.; Ikegami, Y.; Shirakigawa, N.; Ijima, H. Fabrication of liver-derived extracellular matrix nanofibers and functional evaluation in in vitro culture using primary hepatocytes. *Materialia* **2018**, *4*, 518–528. [\[CrossRef\]](#)
96. Kim, Y.; Kim, Y.W.; Lee, S.B.; Kang, K.; Yoon, S.; Choi, D.; Jeong, J. Hepatic patch by stacking patient-specific liver progenitor cell sheets formed on multiscale electrospun fibers promotes regenerative therapy for liver injury. *Biomaterials* **2021**, *274*, 120899. [\[CrossRef\]](#)
97. Wei, J.; Lu, J.; Liu, Y.; Yan, S.; Li, X. Spheroid culture of primary hepatocytes with short fibers as a predictable in vitro model for drug screening. *J. Mater. Chem. B* **2016**, *4*, 7155–7167. [\[CrossRef\]](#) [\[PubMed\]](#)
98. Abdullah CA, C.; Albert, E.L. Carbon nanotubes as biological transporters and tissue-engineering scaffolds. In *Synthesis, Technology and Applications of Carbon Nanomaterials*; Elsevier: Amsterdam, The Netherlands, 2019; pp. 135–156.

-
99. Koga, H.; Fujigaya, T.; Nakashima, N.; Nakazawa, K. Morphological and functional behaviors of rat hepatocytes cultured on single-walled carbon nanotubes. *J. Mater. Sci. Mater. Med.* **2011**, *22*, 2071–2078. [[CrossRef](#)] [[PubMed](#)]
 100. Wei, J.; Lu, J.; Chen, M.; Xie, S.; Wang, T.; Li, X. 3D spheroids generated on carbon nanotube-functionalized fibrous scaffolds for drug metabolism and toxicity screening. *Biomater. Sci.* **2020**, *8*, 426–437. [[CrossRef](#)]
 101. Salerno, S.; Tasselli, F.; Drioli, E.; De Bartolo, L. Poly (ϵ -caprolactone) hollow fiber membranes for the biofabrication of a vascularized human liver tissue. *Membranes* **2020**, *10*, 112. [[CrossRef](#)]

Chemically Modified Dipeptide Based Hydrogel Supports Three-Dimensional Growth and Functions of Primary Hepatocytes

Saikat Biswas, Ashwini Vasudevan, Nitin Yadav, Saurabh Yadav, Preety Rawal, Impreet Kaur, Dinesh M. Tripathi, Savneet Kaur,* and Virander Singh Chauhan*



Cite This: <https://doi.org/10.1021/acsabm.2c00526>



Read Online

ACCESS |



Metrics & More



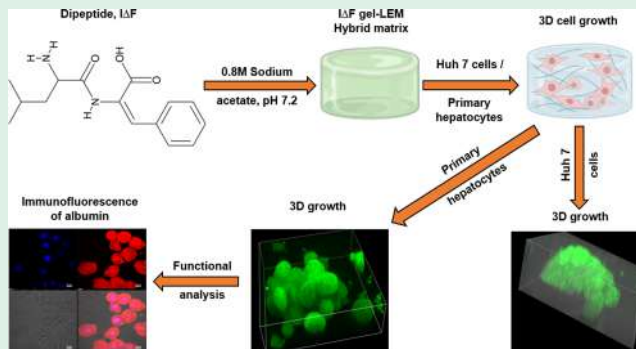
Article Recommendations



Supporting Information

ABSTRACT: A huge shortage of organ donors, particularly in the case of liver, has necessitated the development of alternative therapeutic strategies. Primary hepatocytes (pHCs) transplantation has made a considerable transition from bench to bedside, but the short-term viability and functionality of pHCs in vitro limit their use for clinical applications. Different cell culture strategies are required to maintain the proliferation of pHCs for extended periods. Here, we described the formation of a hybrid scaffold based on a modified dipeptide for the culture of pHCs. First, the dipeptide (Dp), isoleucine- α,β -dehydrophenylalanine (ΔF) was synthesized, purified, and fully characterized. ΔF readily formed a highly stable hydrogel, which was also characterized by CD, TEM, and thioflavin T assay. The addition of soluble liver extracellular matrix (sLEM) to the dipeptide readily formed a hybrid scaffold that was characterized by TEM, and its mechanical strength was determined by rheology experiments. The hybrid scaffold was translucent, biocompatible, and proteolytically stable and, with its mechanical strength, closely mimicked that of the native liver. LEM₁-Dp matrix exhibited high biocompatibility in the readily available adherent liver cell line Huh7 and primary rat hepatocyte cells (pHCs). pHCs cultured on LEM₁-Dp matrix also maintained significantly higher cell viability and an escalated expression of markers related to the hepatocytes such as albumin as compared to that observed in cells cultured on collagen type I (Col I)-coated substrate plate (col-TCTP). Z-stacking of confocal laser microscopy's volume view clearly indicated pHCs seeded on top of the hydrogel matrix migrated toward the Z direction showing 3D growth. Our results indicated that low molecular weight dipeptide hydrogel along with sLEM can resemble biomimetic 3D-like microenvironments for improved pHCs proliferation, differentiation, and function. This hybrid scaffold is also easy to scale up, which makes it suitable for several downstream applications of hepatocytes, including drug development, pHCs transplantation, and liver regeneration.

KEYWORDS: dipeptide hydrogel, extracellular matrix, hybrid scaffold, hepatocytes, tissue engineering



1. INTRODUCTION

The liver performs many essential functions of the body, including glycogen storage, plasma protein production, drug detoxification, and xenobiotic metabolism.¹ Liver diseases impacting over 600 million people are the 16th leading cause of death worldwide.² Liver transplantation is a well-known treatment for end-stage liver disease, and liver failure, but it is severely hampered by the acute shortage of suitable organ donors. The list of patients requiring liver transplantation has outnumbered the list of donor's livers, and only 1 out of 100 deserving liver disease patients finally get a donor's liver.³

Hence, alternative strategies for liver transplantations or effective therapies for end-stage liver diseases are continuously under investigation.⁴ In the past few decades, extracorporeal bioartificial liver (BAL) has been used as a transient support device for patients with liver failure until a suitable graft becomes available.⁵ However, given the limited survival and

replicative ability of primary hepatocyte cells (pHCs) in vitro, BAL therapy has not achieved much clinical success. Short-term viability and functionality of the hepatocytes ex vivo are also one of the major limitations of hepatocyte-based cell therapies.⁶ In addition to mesenchymal stem cells, other stem cell therapies have also been explored as potential treatments for primary hepatocyte cultures, but they cannot replace pHCs.^{7,8}

To facilitate three-dimensional (3D) long-term growth and cultures of primary hepatocytes in vitro, commercially available

Received: June 4, 2022

Accepted: August 11, 2022



polymeric hydrogels such as matrigel and other synthetic scaffolds have been reported.⁹ Polymers of natural origin such as fibrin and collagen have widely been explored for making hydrogel scaffolds to provide enhanced cellular interactions for cell growth applications.¹⁰ However, these hydrogels have several drawbacks, such as they are derived from animal sources and may have variable properties, and there is always a possibility of viral contamination in their preparation. In addition, they may trigger an immune response when introduced to a host and suffer from reproducibility issues.¹¹ During the past two decades, a number of synthetic polymer-based gels, such as poly(ethylene glycol), and polymethacrylamide, have been shown to provide several advantages, such as high water content (>90%), high mechanical strength, and biocompatibility. However, they suffer from several disadvantages including low biodegradability, lack of functional sites for cellular adhesion, and their inability to mimic the natural liver microenvironment completely.¹²

In the past few decades, nanomaterials based on synthetic peptides have attracted a lot of interest because they closely resemble tissue-like consistencies. Peptide-based scaffolds have several advantages such as easy synthesis in large quantities, cost-effectiveness, biocompatibility, nontoxic byproducts by enzymatic degradation, and tunable mechanical stability.^{13,14} Several hydrogel scaffolds based on relatively large peptides have been explored earlier for 3D cell culture applications. For example, RADA-16-based hydrogels were used to culture hepatocytes.¹⁵ However, these peptides-based hydrogels suffer from various disadvantages, including relatively complex design, synthesis, and characterization, high cost, and difficulty in mimicking the liver microenvironment.¹⁶ In the past few decades, many short peptides (2–5 residues) have been shown to self-assemble into different hierarchical nanostructures.¹⁷ Recent findings that ultrashort peptides such as dipeptides can form fibrillar gel-like nanostructures have made this field of research immensely attractive.¹⁸ Dipeptides containing naturally occurring L-amino acids, including LF, IF, and Fmoc-FF, have been investigated for their self-assembly into fibrillar gel-like structures.^{17–20} However, peptide-based hydrogels containing L-amino acids generally suffer from proteolytic instability, which makes them relatively unsuitable for in vivo applications.^{12,21,22} To address this concern, the strategy of using nonprotein amino acids, including D-amino acids and α -substituted amino acids in the peptide sequence has been adopted by many researchers.^{17,18} For example, de Groot et al. have evaluated the ability of a set of dipeptides containing both L- and D-amino acids to form fibrillar structures.¹⁹ We have previously shown that the introduction of ΔF in the peptide sequence confers conformational constraints in the peptide backbone and induce proteolytic stability. We have also shown that dipeptides consisting of α,β -dehydrophenylalanine (ΔF) at their carboxyl terminal readily formed a variety of stable nanosized structures such as spherical, tubular, and fibrillar structures.^{23–32}

In the present study, we have described the preparation of a hybrid scaffold and explored its suitability for the culture of pHCs to maintain hepatocyte functions in in vitro conditions. A dipeptide (Dp) containing isoleucine and α,β -dehydrophenylalanine (ΔF) was synthesized, and its gelation properties were explored in different conditions. ΔF formed a mechanically strong hydrogel at 1 wt % peptide concentration. In an earlier study, we also have shown that ΔF can form micellar structures at lower concentrations (0.2 wt %).³³ It has

been recently shown that liver extracellular matrix (LEM) coating can create a favorable microenvironment for pHCs in vitro.³⁴ Proteins present in the LEM are known to provide a physical substratum for cellular adhesion and help to maintain hepatic functions.³⁵ To mimic the liver microenvironment, a hybrid hydrogel (LEM-Dp) containing Dp gel with soluble liver extracellular matrix (sLEM) was prepared to grow the culture of primary hepatocytes. The hybrid hydrogel was found to preserve the functionality of freshly isolated pHCs and represent a better alternative for the growth of primary liver cells with in vitro conditions for extended periods.

2. MATERIALS

Boc-Ile-OH was obtained from Novabiochem. This study was conducted using Sigma-Aldrich, St. Louis, MO, USA products including trifluoroacetic acid, sodium bicarbonate, ammonium hydroxide, triisopropylsilane, tetrahydrofuran, N-methyl morpholine, isobutyl chloroformate, DL-3-phenylserine hydrate, dimethyl sulfoxide, sodium chloride, anhydrous sodium acetate, sodium hydroxide, and 4-(2-hydroxyethyl)-1-piperazineethanesulfonic acid. Acetic anhydride was purchased from SD Fine Chem Ltd., Mumbai, India. Merck, Darmstadt, Germany, provided the following materials: ethyl acetate, HPLC grade acetonitrile, 1-propanol, DAPI, anhydrous sodium sulfate, methanol, anhydrous diethyl ether, and dimethylformamide. The following chemicals were provided by Himedia, Mumbai, India: trypsin EDTA, phosphate buffer saline, citric acid, endotoxin-free water, trypan blue, fetal bovine serum (FBS), 3-(4, 5-dimethylthiazol-2-yl)-2,5-diphenyltetrazolium bromide, and gentamycin. Confocal dishes were purchased from ibidi (Gewerbehof Gräfelfing). We obtained the following materials from Thermo Fisher Scientific: penicillin–streptomycin, calcein AM, Pierce BCA Protein Assay Kit, and Dulbecco's modified Eagle's medium. The primary antibody (sc-271605) was obtained from Santa Cruz Biotechnology, Santa Cruz, CA, USA. β -Actin (4967S) antibody was obtained from Cell Signaling Technology (Danvers, MA, USA). Secondary antibodies 11032 and A11037 were obtained from Invitrogen (Waltham, MA, USA).

3. METHODS

3.1. Synthesis and Characterization of the Dipeptide, ΔF .

3.1.1. Solution Phase Peptide Synthesis. The method of synthesis of isoleucine- α,β -dehydrophenylalanine (ΔF) has been outlined in [Supporting Information](#) Text S1, while chemical reactions involved in the synthesis are provided as a schematic representation in [Supporting Information](#) Figure S1.^{24–29} The dipeptide was characterized using RP-HPLC (Shimadzu, pump-LC-10AT, PDA Detector, autosampler-SIL-10AD) and a Phenomenex C-18 column. A binary gradient of methanol–water (5–95%, 0.1% TFA) mobile phase at a flow rate of 1 mL/min for 45 min was used. Electron spray ionization mass spectrometry (ESI-MS) Thermo Proteome Discover 2.2.0.388 was used to determine the molecular mass of the dipeptide (0.1 mg/mL dipeptide in LC-MS grade acetonitrile and 0.1% formic acid).

3.1.2. Infrared Spectroscopy. For Fourier transform Infrared spectroscopy (FT-IR) of ΔF , PerkinElmer FT-IR/NIR spectrometer was used (Frontier MIR + SP10 STD). Lyophilized peptide powder was placed on the PerkinElmer Universal ATR sample holder. The wave number was taken at 400–4000 cm^{-1} .

3.2. Animal Ethics Statement. Animal experiments were performed according to the guidelines of the Institutional Animal Ethics committee (IAEC), Centre for comparative medicine, Institute of Liver and Biliary Sciences, Delhi. The animal ethics committee duly approved the study of ILBS (IAEC/ILBS/19/12).

3.3. Decellularization of Rat Liver. For decellularization, Sprague–Dawley (SD) rat (male, 8 weeks) was anesthetized by intraperitoneal injections of a ketamine (75–100 mg/kg body weight) + xylazine (10–12 mg/kg body weight) cocktail. In the anesthetized animals, the portal vein was exposed and cannulated as previously reported.³⁶ First, the detergents, including 1% Triton-X 100 with 0.1% ammonium hydroxide, were perfused through the portal vein for

about 20–24 h to decellularize the liver, which was then followed by PBS for 4 h to wash the detergents thoroughly. Once decellularized, the liver samples were lyophilized further to obtain dried LEM and stored in an airtight container for further use.

3.4. Histological Characterization and DNA Quantification of the Decellularized Liver. Characterization of decellularization was performed by histological and DNA analysis. Liver tissue slices cut from decellularized livers were fixed and embedded in paraffin, deparaffinized, and then stained with hematoxylin and eosin (H&E). The DNA content was quantified from a part of the decellularized liver and a control native rat liver using a nanospectrophotometer at 260 nm, as reported earlier.³⁶

3.5. Digestion of Decellularized Rat Liver and Quantification of Proteins. As reported earlier, the decellularized liver samples were crushed into powder form and performed with minor modification.³⁷ Briefly, (5 mg of LEM powder):(1 mL of 0.5 M acetic acid):(2 mg of pepsin) was added under constant stirring at 37 °C until no traces of powder were visible and a homogeneous solution was formed. After pepsin solubilization, the whole solution was centrifuged and the supernatant collected and lyophilized. The lyophilized powder was dissolved in the desired amount of sterile water and the soluble protein quantitated using Pierce BCA Protein Assay Kit (Thermo Scientific) according to the manufacturer protocol. VersaMax ELISA reader (Molecular Devices, Sunnyvale, CA, USA) was used to measure the absorbance of the samples at 540 nm. Lyophilized and soluble protein was run on SDS-PAGE on a 10% acrylamide gel.

3.6. Protein Identification of Decellularized Rat Liver Using LC/MS-MS. Freshly prepared dithiothreitol (DTT) was added to a 40 μ g of protein solution (protein in 50 mM ammonium bicarbonate solution, pH 8) so that the final concentration of DTT would be 5 mM and incubated for 1 h at 60 °C. Then freshly prepared iodoacetamide (IAA) was added to reach the above solution's final concentration of 20 mM and incubated for 30 min in dark at room temperature. Then 2 μ g of trypsin (20:1 protein:trypsin, pH 8) was added and incubated for 24 h at 37 °C in a water bath. Formic acid was added to bring the pH to 3 to stop the reaction. The supernatant was collected in a fresh tube after centrifuging at 12,000 rpm for 15 min and vacuum-dried. Zip tip was performed by resuspending in 1% formic acid solution, vacuum-drying, resuspending in mass spec solvent (solvent A), and injecting into LC/MS-MS. Proteome Discoverer 2.4 was used for the analysis of raw files. A basic SequestHT search against *Rattus norvegicus* database (acquired from UniProt) was performed with high-confidence peptide filters for peptide identification.

3.7. Formation of Dp Gel. IΔF solubility was checked in different solvents such as methanol and 1-propanol, and self-assembly behavior was investigated using different buffers (sodium acetate, pH 7.2; 0.1 M sodium citrate, pH 6.1; carbonate–bicarbonate buffer, pH 9.5) and details in Supporting Information Table S3. Finally, 1 mg of Dp was dissolved in 30–50 μ L of 1-propanol using 10 min sonication. Dp hydrogel at a concentration of 1 wt % was formed by adding 0.8 M sodium acetate buffer (pH 7.2–7.4) to the peptide solution at room temperature. A tube inversion test for gels prepared in 1.7 mL Eppendorf tubes was performed to determine mechanical stability of gel structures.

3.8. Circular Dichroism Spectroscopy. Circular dichroism (CD) spectroscopy experiments were carried out at 0.1–1 mg/mL peptide concentration prepared in 0.8 M sodium acetate buffer, and details of the experimental procedure have been described earlier.¹²

3.9. Thioflavin T Fluorescence Assay. Thioflavin T fluorescence assay was performed on Dp at 0.1–1 mg/mL peptide concentrations and monitored using an ELISA reader (VersaMax, Molecular Devices; excitation—440 nm; emission—482 nm). Thioflavin T dye was added (2 μ L/(200 μ L of sample); stock, 2 mM) to the samples, and a reading was taken after 30 min.¹²

3.10. Proteolytic Stability of Dp Gel In Vitro. To test the proteolytic stability of the Dp gel, freshly prepared 100 μ L of gel (1 wt %) was treated with proteinase K (1:10 Dp gel:enzyme, w/w), FBS (10% FBS, v/v), Huh 7, and primary hepatocytes culture supernatant

(1:1 Dp gel:culture supernatant, v/v), and the procedure was also described in earlier literature.^{12,22,23} The stability of dipeptide was monitored using RP-HPLC (Shimadzu, pump-LC-10AT, PDA Detector, autosampler-SIL-10AD) with a gradient of methanol–water (5–95%, 0.1% TFA) on a Phenomenex C-18 column (flow rate of 1 mL/min for 45 min).

3.11. Preparation of IΔF Hybrid Matrix (LEM-Dp). To prepare the IΔF hybrid matrix, soluble liver extracellular matrix (sLEM) was added to 1 wt % Dp gel at different concentrations, 0.15 mg/mL (LEM₁-Dp), 0.3 mg/mL (LEM₂-Dp), and 0.45 mg/mL (LEM₃-Dp), at room temperature. Three LEM-Dp hybrid matrices were allowed to stabilize in undisturbed conditions overnight.

3.12. Mechanical Strength of LEM-Dp Matrix. To determine the strength of 1 wt % Dp gel, LEM₁-Dp matrix, LEM₂-Dp matrix, and LEM₃-Dp matrix rheological studies were performed using an MCR 102e (Anton Paar, parallel plate geometry of diameter 25 mm was used), and a detailed experimental procedure can be found in literature published previously.^{12,38}

3.13. Morphological Analysis of LEM₁-Dp Matrix and Its Stability. The morphologies of 1 wt % Dp gel and LEM₁-Dp matrix were analyzed using the 120 kV mode of TEM (Tecna 12 BioTWIN, FEI Netherlands), micrographs were taken using Analysis II (Megaview, SIS, Germany) software, and the detailed experimental procedure has been described earlier.^{30,38}

The microstructural features of the 1 wt % Dp gel and LEM₁-Dp matrix were determined using SEM, and images were acquired using a Carl Zeiss scanning electron microscope (Model EVO LS10). SEM was equipped with a lanthanum hexaboride emitting cathode and SmartSEM operating software.¹²

Frequency sweep rheology experiment was carried out for LEM₁-Dp matrix to investigate its stability under mechanical stress within the linear viscoelastic region (Anton Paar MCR 102e, parallel plate geometry of diameter 25 mm was used).^{12,38}

A time sweep rheology study was also carried out to evaluate the mechanical stability of LEM₁-Dp matrix with time. The changes in storage modulus (G') and loss modulus (G'') values were recorded as a function of time up to 50 min (Anton Paar MCR 102e, parallel plate geometry of diameter 25 mm was used).

3.14. Morphological Characterization of LEM₁-Dp Matrix under Culture Conditions. Scanning electron microscope imaging (Carl Zeiss, Model EVO LS10) of LEM₁-Dp matrix treated with Huh7 cells and pHCs culture supernatant (37 °C, 7 days) was used to monitor morphological changes in the gel structure as described earlier.^{30,38}

3.15. Cell Culture. Huh7 cells were cultured in a complete medium (CDMEM, 10% FBS, 0.1% penicillin–streptomycin) and maintained in a humidified incubator (37 °C, 5% CO₂). The cells were passaged when they reached a confluency level of 70–80%.

3.16. Primary Hepatocyte Isolation and Characterization. For pHCs isolation, the protocols were followed as per our previous studies.³⁹ Briefly, the animals were anesthetized with ketamine and xylazine, and the liver was exposed by making an incision in the upper abdomen. A 200 μ L aliquot of Hanks's buffer solution was injected at a perfusion rate of 20 mL/min into the portal vein via a 24-gauge catheter while leaving the inferior vena cava open as an outlet flow. Next, for in vivo enzymatic digestion, 150 mL of Hanks buffer containing 30 mg of collagenase type 1 was injected with the perfusion rate of 5 mL/min, and the inferior vena cava was ligated with the help of thread. The perfused liver was then excised from the animal, minced, and transferred to 100 mL of Hanks buffer containing 10 mg of collagenase at 37 °C for in vitro digestion. The perfusate was filtered by a 100 μ m nylon strainer and centrifuged at 50 g for 5 min at 4 °C. The pellet was washed twice in DMEM containing 10% FBS and analyzed for viability using trypan blue stain. Hepatocytes with cell viability greater than 80% were cultured. About 4.5×10^6 cells were plated in DMEM-F12 containing 10% FBS and 1% ITS (insulin transferrin selenium) for 6–12 h for adherence, followed by culturing in DMEM-F12 containing 1% ITS in six-well plates. They were characterized by the expression of albumin on day 2 after isolation, as earlier reported. Briefly, the cells were fixed with 4% paraformaldehyde

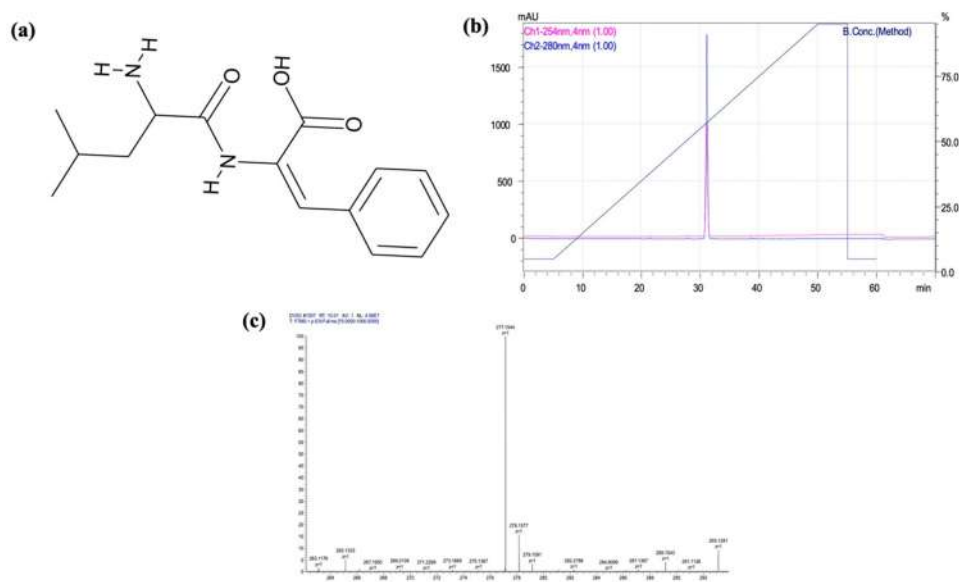


Figure 1. (a) Chemical structure of IΔF. Characterization of IΔF. (b) RP-HPLC profile of IΔF showing a single peak at RT, 31 min, and a 5–95% gradient of methanol–water. (c) Mass spectrum of IΔF showing the mass of 277.15 Da ($276 + {}^1\text{H}^+$).

hyde, washed, treated with blocking buffer (1 mg/mL BSA in PBS), and then incubated with primary albumin antibody (elabsciences, 1:200 in blocking buffer) at 4 °C overnight. Following PBS washes, they were incubated with rhodamine-labeled secondary antibody (1:500 in blocking buffer) at room temperature for 45 min and then stained with DAPI (Life Technologies, Carlsbad, CA, USA) and imaged using a fluorescence microscope (Nikon, Minato City, Tokyo, Japan).

3.17. Viability of Huh7 Cells and pHCs on the LEM-Dp Hybrid Matrix. Huh7 cells were cultured in DMEM supplemented with 10% fetal bovine serum and 0.1% penicillin–streptomycin in the CO₂ incubator. The freshly prepared LEM₁-Dp matrix, LEM₂-Dp matrix, and LEM₃-Dp matrix were washed with PBS and an incomplete medium. Subconfluent Huh7 cells were harvested by trypsinization and washed with PBS and complete media. Cells at a concentration of 1×10^4 cells/well were plated in a 96-well plate and incubated with LEM₁-Dp matrix, LEM₂-Dp matrix, LEM₃-Dp matrix, and TCTP plate as a positive control for 72 h. The cell viability of Huh7 was tested using a standard 3-(4,5-dimethyl thiazolyl-2)-2,5-diphenyltetrazolium bromide (MTT) assay as described earlier.³¹ Freshly isolated pHCs were seeded at 2.5×10^4 cells/well in LEM₁-Dp and co-TCTP in a 96-well plate. The cell viability of pHCs was also checked by MTT assay as described above.

3.18. Live–Dead Viability Assay of Huh7 Cells and pHCs on LEM₁-Dp Matrix. Huh7 cells (10×10^3 /confocal dish) and pHCs (10^5 /confocal dish) were seeded on LEM₁-Dp matrix and incubated in a humidified incubator (5% CO₂, 37 °C) for 2, 3, 5, and 7 days. The culture medium was discarded, and cells were stained with 2 μM calcein AM dye solution and incubated with the dye solution for 45–60 min to facilitate the detection of viable cells inside the gel matrix. For confocal microscopy imaging, confocal laser scanning (Nikon A1r) under a Nikon microscope (Nikon, Minato City, Tokyo, Japan) (objective plane Apo 60/1.4 oil) was used. The final images were processed and assembled using NIS Elements (Nikon). Three-dimensional images were generated from a Z-stack of laser confocal microscopy scans of 1 μm increments over the total thickness of 100 μm, and a detailed procedure was described in earlier literature.²³

3.19. Albumin and Urea Analysis of Huh7 Cells and pHCs in Culture Supernatant. We measured the concentrations of albumin and urea, two well-known indicators of hepatocyte activity, in the cultivated Huh7 and primary hepatocyte cells' supernatants. Conditioned medium was collected and stored at –80 °C until further analysis. Albumin and urea were measured in cell soups using

commercially available quantitative colorimetric ELISA kits (Sigma-Aldrich) as per the manufacturer's instructions.

3.20. Immunofluorescence Analysis of pHCs. Expression of albumin by pHCs on days 2, 3, 5, and 7 was assessed using immunofluorescence analysis. The cells were fixed with 500 μL of 4% paraformaldehyde and were permeabilized using 500 μL of 1% Tween 20 in PBS for 10 min. Cells were then treated with 2 mL of blocking buffer (1× PBS + 0.3% Tween 20 + 2% BSA) for 2 h and then incubated with 2 mL of diluted primary albumin antibody (sc-271605; antibody to dilution buffer, 1:500) in dilution buffer (1× PBS + 0.3% Tween 20 + 0.5% BSA) at 4 °C overnight. Following three washes with a wash buffer of 2 mL each (1× PBS + 0.3% Tween 20), cells were incubated with 2 mL of diluted Alexa fluor labeled secondary antibody (A 11032; antibody to dilution buffer, 1:500) for albumin at room temperature for 2 h. After four washings (2 mL/wash), cells were stained with DAPI (DUO82040) as per the given instructions by the manufacturer and imaged using confocal laser scanning (Nikon A1r) under a Nikon microscope (Nikon, Minato City, Tokyo, Japan). Image processing was conducted with NIS Elements (Nikon) for the final image assembly.

3.21. Statistics. Data were analyzed using the GraphPad Prism Software, version 6.01 (San Diego, CA, USA). The results are presented as mean ± standard deviation (SD).

4. RESULTS

4.1. Synthesis and Characterization of the Dipeptide, IΔF. Solution-phase peptide synthesis method was adopted to synthesize IΔF. The synthesized peptide was characterized using RP-HPLC, which was eluted as a single peak at 31 min (Figure 1b). Mass spectrometry result showed a molecular weight of 277.15 Da (Figure 1c). These results clearly showed that the peptide was more than 95% pure. The peptide was also characterized using FT-IR, which showed peaks for amide-I, amide-II, and amide-III regions at 1691, 1492, and 1255 cm^{–1}, respectively. (Supporting Information Figure S2).

4.2. Decellularization, Characterization, and Solubilization of Rat Liver. Decellularization of the native liver through portal vein cannulation and the perfusion of detergents resulted in a shiny white appearance after 48 h of the decellularization process, indicating complete removal of the liver cells (Figure 2a,b). Characterization of the

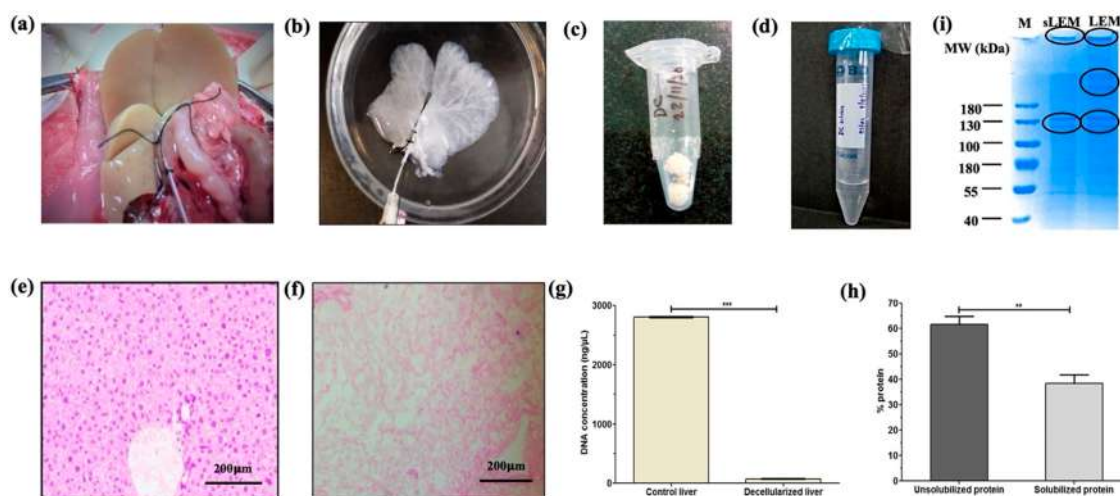


Figure 2. (a) Native rat liver with portal vein cannulation. (b) Native rat liver after decellularization. (c) Lyophilized decellularized rat liver sample. (d) Solubilized liver (pepsin soluble) extracellular matrix (sLEM). Histological characterization of the liver: (e) H&E of native rat liver and (f) H&E of decellularized rat liver. (g) Quantification of dsDNA of native rat liver and decellularized rat liver. (h) Digestion of decellularized liver and quantification of soluble proteins. (i) 10% SDS-PAGE: molecular marker (M), pepsin soluble liver extracellular matrix (sLEM), and lyophilized powder of liver extracellular (LEM). Error bar for each point is the mean \pm standard deviation; *** $p < 0.0001$, and ** $p < 0.001$.

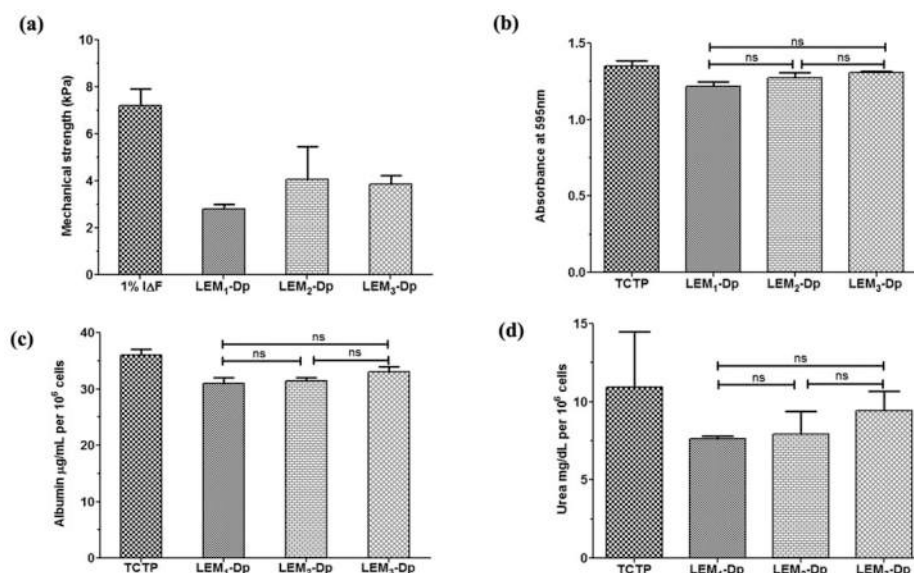


Figure 3. (a) Mechanical strength of 1 wt % IΔF, LEM₁-Dp matrix, LEM₂-Dp matrix, and LEM₃-Dp matrix at 0.8 M sodium acetate buffer (pH 7.2). (b) Viability of Huh7 cells cultured on TCTP and LEM₁-Dp matrix, LEM₂-Dp matrix, and LEM₃-Dp matrix using MTT assay. Hepatocytes functional analysis: (c) levels of albumin and (d) urea produced by Huh7 cells cultured on TCTP and LEM₁-Dp matrix, LEM₂-Dp matrix, and LEM₃-Dp matrix on day 3. Error bar of each point is the mean \pm standard deviation, and ns = nonsignificant ($p > 0.05$).

decellularized liver was performed to assess the efficiency of decellularization. The hematoxylin and eosin (H&E) histology-based microscopic analysis showed that no cells were present in the decellularized liver in contrast to the native liver (Figure 2e,f).

DNA content experiments also revealed the absence of cell nuclei and hence a reduction in the DNA in the decellularized liver as compared to the native liver (2800 ± 1.2 to 69 ± 0.3 ng/μL, *** $p < 0.0001$ (Figure 2g)). The lyophilized LEM liver was partially solubilized using pepsin (Figure 2c,d). The yield of solubilized LEM (sLEM) protein was about $38.46 \pm 3.38\%$, ** $p < 0.001$ (Figure 2h). In SDS-PAGE, different bands for the molecular weight distribution of pepsin-digested sLEM and lyophilized LEM powder were observed. Different molecular

weight bands were confirmed above as 70 kDa (~ 220 , ~ 210 , ~ 130 , and ~ 120 kDa) in both LEM and sLEM (Figure 2i). LC/MS-based analysis of sLEM identified 149 proteins (Supporting Information Table S1) of *Rattus norvegicus* with high-confidence peptide filters for peptide identification.

4.3. Formation of Dp Gel. Self-assembling properties of Dp at different peptide concentrations (0.3, 0.5, 0.7, 0.9, and 1 wt %) into hydrogel were evaluated in different solvent–buffer combination systems which have been widely used in the literature. Dp was dissolved in solvents such as methanol and 1-propanol, followed by the addition of buffers including 0.8 M sodium acetate, pH 7.2; 0.1 M sodium citrate, pH 6.1; and carbonate–bicarbonate buffer, pH 9.5 (Supporting Information Table S2). The formation of a mechanically strong

semisolid gel-like structure that can withstand gravitational forces was observed in the tube inversion test. This test showed that the gelation occurred in all of the above conditions starting from 0.5 wt % peptide concentration in the case of peptide dissolved in methanol, and 0.7 wt % in the case of 1-propanol. However, the formation of gel was instantaneous in the case of 0.8 M sodium acetate, pH 7.2 buffer, and therefore, this was chosen for further studies (Supporting Information Figure S3).

4.4. Circular Dichroism Spectroscopy. The secondary structure of Dp gel at several concentrations (0.1–1 wt %) was investigated in 0.8 M sodium acetate, pH 7.2. CD spectra depicted a positive band at 212 nm and a negative band at 270 nm (Supporting Information Figure S4a). There were no changes in ellipticity for Dp at different peptide concentrations.

4.5. Thioflavin T Fluorescence Assay. Thioflavin T fluorescence experiment was utilized to monitor the process of fibrillization at different peptide concentrations (0.1–1 wt %). An increase in fluorescence intensity with increasing peptide concentration was observed, which indicated peptide concentration-dependent self-assembly of the peptide (Supporting Information Figure S4b).

4.6. Proteolytic Stability of Dp Gel. The stability of Dp gel was evaluated in the presence of a nonspecific protease (Proteinase K) and cocktails of several proteases (present in FBS, Huh 7 cells, and pHCs culture supernatants). RP-HPLC chromatograms for Dp gels treated with the above-mentioned proteases showed no changes in the retention time of the peptide in any conditions (Supporting Information Figure S5 and Table S3).

4.7. LEM-Dp Hybrid Matrix Preparation and Its Characterization. Three hybrid matrices were prepared consisting of Dp gel (1 wt %) containing different sLEM concentrations of 0.15, 0.3, and 0.45 mg/mL (LEM₁-Dp matrix, LEM₂-Dp matrix, and LEM₃-Dp matrix, respectively). Rheological amplitude sweep experiments were conducted to evaluate the mechanical strengths of the three hybrid matrices. The mechanical strengths (G') of 2.8 ± 0.2 , 4.05 ± 1.40 , and 3.87 ± 0.36 kPa for LEM₁-Dp matrix, LEM₂-Dp matrix, LEM₃-Dp matrix, respectively, were observed, while Dp gel alone showed mechanical strength of 7.2 ± 0.71 kPa (Figure 3a and Supporting Information Figure S6a). There were no major changes in mechanical strengths for the three hybrid matrices.

4.8. Cellular Viability and Functional Evaluation of Huh7 Cells Cultured on LEM-Dp Matrices. We evaluated the viability and functionality of Huh7 cells cultured on the three hybrid matrices. Results of the MTT assay showed optical densities (OD) of 1.21 ± 0.04 , 1.27 ± 0.04 , and 1.30 ± 0.01 for Huh7 cells cultured on LEM₁-Dp matrix, LEM₂-Dp matrix, and LEM₃-Dp matrix, respectively ($p > 0.05$). Huh7 cells grown on a TCTP plate, considered to be a gold standard for in vitro culture, showed an OD value of 1.34 ± 0.05 (Figure 4b). Next, the functionality of Huh7 cells cultured on hybrid matrices was evaluated by measuring the levels of albumin and urea secretion by the cells. Huh7 cells cultured on the hybrid matrices for 3 days showed albumin levels of 31 ± 0.01 , 30 ± 0.007 , and 33 ± 0.01 $\mu\text{g/mL}/(10^6 \text{ cells})$ for LEM₁-Dp matrix, LEM₂-Dp matrix, and LEM₃-Dp matrix, respectively ($p > 0.05$) (Figure 3c). Urea levels for the cells cultured on hybrid matrices were 7.65 ± 0.21 , 7.95 ± 2.05 , and 9.45 ± 1.76 mg/dL/ (10^6 cells) for LEM₁-Dp matrix, LEM₂-Dp matrix, and LEM₃-Dp matrix, respectively ($p > 0.05$) (Figure 3d). As there were no major changes in mechanical strength, cell viability,

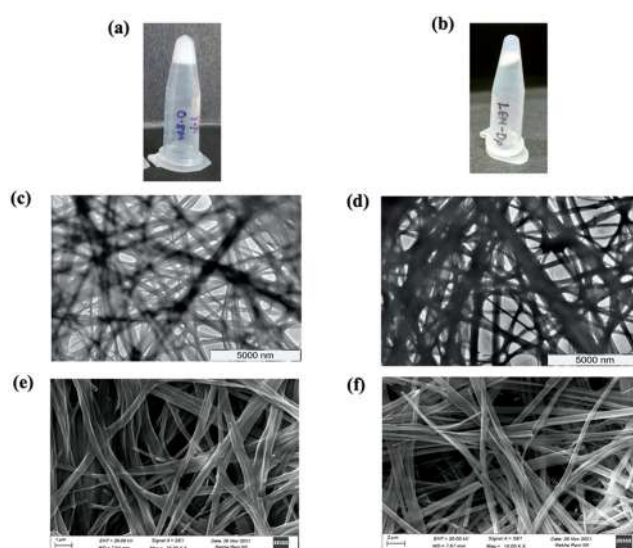


Figure 4. Tube inversion test showing gelation of (a) 1 wt % ΔF hydrogel and (b) LEM₁-Dp matrix in 1-propanol–0.8 M sodium acetate buffer (pH 7.2). Transmission electron microscopy images of (c) 1 wt % ΔF and (d) LEM₁-Dp matrix formed in 1-propanol–0.8 M sodium acetate buffer (pH 7.2). Scanning electron microscopic images showing the topography of (e) 1 wt % ΔF and (f) after adding sLEM with 1 wt % Dp gel (LEM₁-Dp matrix).

and albumin and urea secretion among the three hybrid matrices, we chose the hybrid matrix with the lowest sLEM concentration (LEM₁-Dp matrix) for further experiments.

4.9. Morphological Analysis of LEM₁-Dp Matrix and Its Stability. Morphological characteristics of the gel matrices were investigated using electron microscopy (Figure 4a,b). TEM images for LEM₁-Dp matrix as well as Dp gel depicted the presence of a dense fibrillar mesh with fibril's length in micrometer ranges and ~ 200 – 500 nm diameter (Figure 4c,d). The morphological properties of Dp gel and LEM₁-Dp matrix were also evaluated using SEM, which showed that both gels had interconnected mesh-like dense networks of fibrils (Figure 4e,f).

The stability of LEM₁-Dp matrix was investigated using a rheological frequency sweep experiment which suggested that both G' and G'' values for the matrix were independent of change in the angular frequency, indicating its high stability (Supporting Information Figure S6b). The stability of LEM₁-Dp matrix was also investigated using a time sweep rheology assay, and no observable changes in G' and G'' values with time were observed, which further indicated the high stability of the matrix (Supporting Information Figure S6c).

4.10. Morphological Characterization of LEM₁-Dp Matrix under Culture Conditions. To investigate whether the 3D fibrillar mesh of the hybrid matrix was stable under culture conditions, Huh7 cells and pHCs were grown on the matrix for 7 days, and its stability was monitored using SEM. As expected, no observable changes in the dense fibrillar mesh of the matrix were observed (Supporting Information Figure S7). However, the formation of small spike-like structures observed throughout the gel may be due to the disintegration of the matrix with time.

4.11. Culture of Huh7 Cells on LEM₁-Dp Matrix. To investigate whether the hybrid matrix supports the 3D culture of Huh7 cells in its matrix for longer periods, cell viability, morphology, and functionality of cells cultured in the matrix

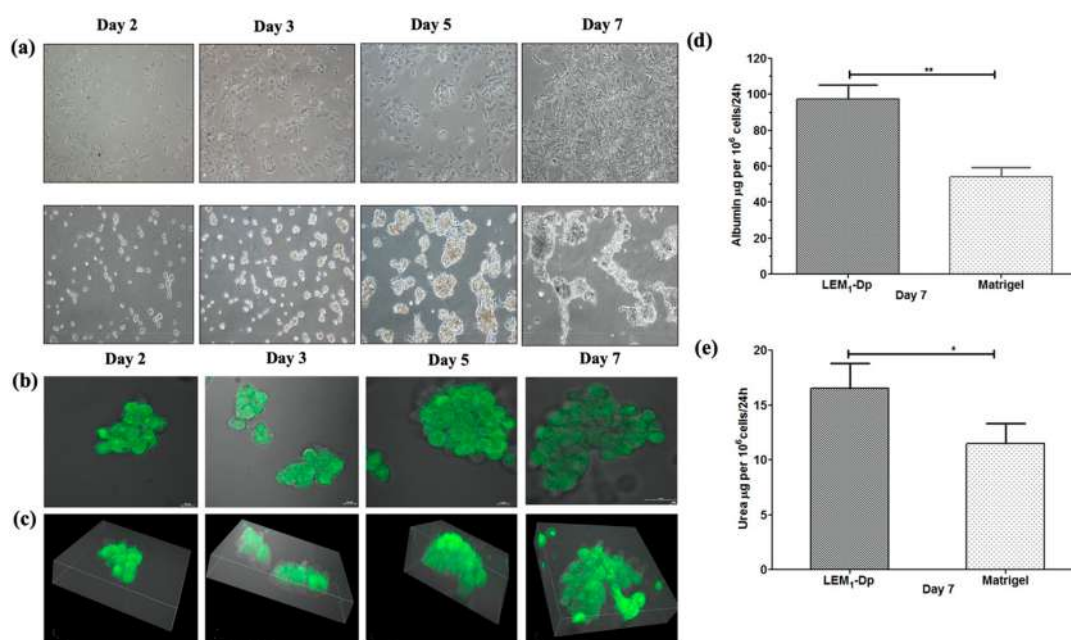


Figure 5. (a) Representative images of bright-field microscopy of Huh7 cells (10× magnification) cultured on LEM₁-Dp matrix on days 2, 3, 5, and 7. Matrigel was used as a control. (b) Representative images of live/dead stain (Calcein-AM) of Huh7 cells, cultured on LEM₁-Dp matrix on days 2, 3, 5, and 7 using confocal laser microscopy at 100× magnification. (c) Representative images of Z-stacking volume view of Huh7 cells stain with calcein-AM, cultured on LEM₁-Dp matrix on days 2, 3, 5, and 7 using confocal laser microscopy at 100× magnification. Hepatic functional analysis of Huh7 cells cultured on LEM₁-Dp matrix and Matrigel at day 7, (d) levels of albumin, and (e) levels of urea. An error bar represents the mean \pm standard deviation; ** $P < 0.001$, and * $P < 0.01$.

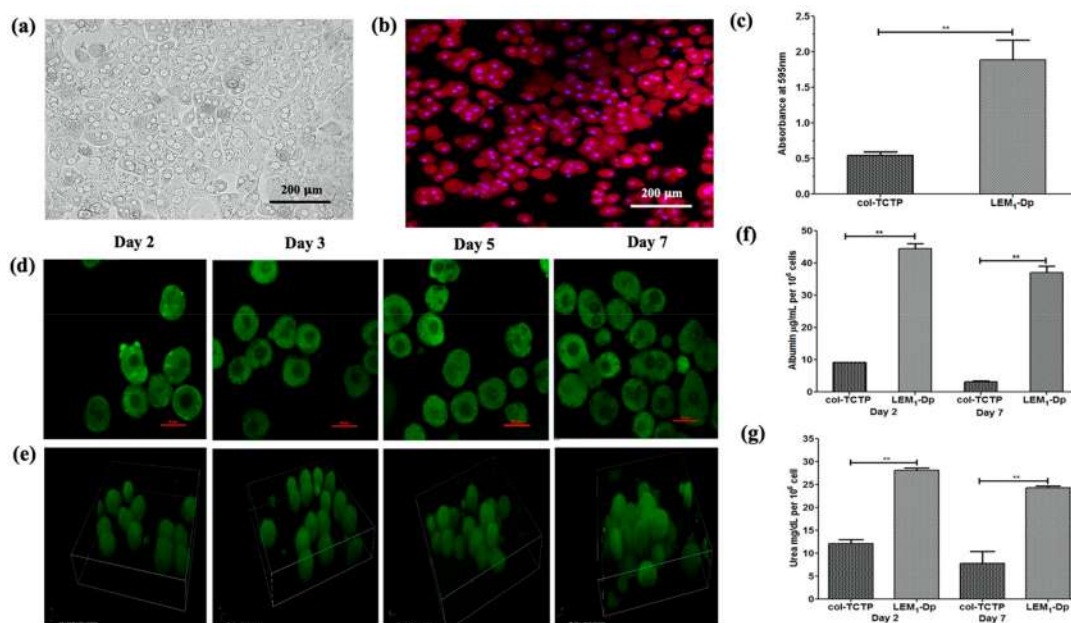


Figure 6. (a) Representative bright-field microscopy image of pHcs freshly isolated from female Sprague–Dawley rats (8 weeks old). (b) Immunofluorescence characterization of freshly isolated rat hepatocytes. (c) Cytotoxicity of freshly isolated primary hepatocytes cultured on LEM₁-Dp matrix using MTT assay. col-TCTP was used as a control. (d) Representative images of confocal laser microscopy of live/dead stain (calcein-AM) of pHcs cultured on LEM₁-Dp matrix observed on days 2, 3, 5, and 7 at 100× magnification. (e) Representative Z-stacking volume view of live/dead stain (calcein-AM) of pHcs, cultured on LEM₁-Dp matrix on days 2, 3, 5, and 7 using confocal laser microscopy at 100× magnification. Functional characterization of pHcs, (f) Albumin levels and (g) urea in culture supernatant on days 2 and 7 cultured on LEM₁-Dp matrix and col-TCTP. Error bar for each point is the mean \pm standard deviation; ** $p < 0.001$.

were monitored. Cellular growth of Huh7 cells cultured on LEM₁-Dp matrix was recorded using light microscopy imaging on days 2, 3, 5, and 7 (Figure 5a). Matrigel, a commercially available protein-based gel for 3D culture applications, was

used as a positive control. On days 1–3, Huh7 cells grew faster to form cell clusters with their adjacent cells, and there were no observable cell morphological changes in LEM₁-Dp matrix and Matrigel groups. During days 5–7, hepatocytes formed more

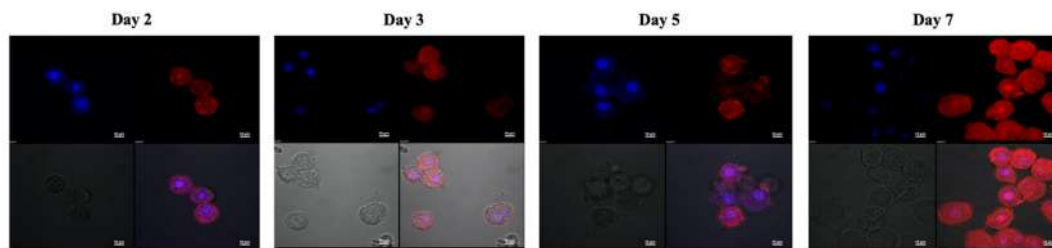


Figure 7. Representative images of pHCs cultured on the LEM₁-Dp matrix showing red fluorescence stain for albumin production on days 2, 3, 5, and 7. Cell nuclei were stained with DAPI (blue) and obtained by confocal laser microscopy at 100× magnification.

prominent clusters and provided more recognizable morphological characteristics in 3D culture conditions of both gels. Next, Huh7 cells cultured on LEM₁-Dp matrix were stained with live cell staining dye, i.e., calcein-AM, and imaged using a fluorescence confocal microscope to investigate changes in cell morphology and viability. High green fluorescence for cells cultured in the matrix for 7 days indicated the healthy and viable nature of the cells in clustered morphology (Figure 5b). Three-dimensional projections during confocal microscopy allowed cell proliferation analysis via Z-stack imaging, which indicated that the viable cell clusters were present throughout the matrix (green fluorescence due to calcein-AM stain) (Figure 5c). Hepatic functions of Huh7 cells cultured on LEM₁-Dp matrix for day 7 were also evaluated by measuring albumin and urea secretion levels in the cells. Huh7 cells cultured on LEM₁-Dp matrix secreted albumin $97.6 \pm 7.6 \mu\text{g}/(10^6 \text{ cells})$ as compared to Matrigel $54.3 \pm 4.9 \mu\text{g}/(10^6 \text{ cells})$, $^{**}p < 0.001$ (Figure 5d). Urea levels for the cells cultured on LEM₁-Dp matrix and Matrigel were $16.52 \pm 2.3/(10^6 \text{ cells})$ and $11.51 \pm 1.8/(10^6 \text{ cells})$, respectively, $^{*}p < 0.01$ (Figure 5e).

4.12. Culture of pHCs on LEM₁-Dp Matrix. Next, we evaluated whether LEM₁-Dp matrix supports the culture of pHCs. For this, pHCs were isolated from rat liver, and the viability was more than 80%. More than 70% of the cells were adherent to a collagen-coated plate within 2 h after plating (Figure 6a). The isolated hepatocytes were also characterized using albumin staining, and we observed albumin-positive cells for day 2 culture (Figure 6b). In order to examine the viability of pHCs cultured on LEM₁-Dp matrix, we first carried out an MTT assay. col-TCTP, a gold standard for pHCs culture, was used as a control. OD values of 1.88 ± 0.28 and 0.54 ± 0.05 were observed for pHCs grown on LEM₁-Dp matrix and col-TCTP, respectively, $^{*}p < 0.001$ (Figure 6c). The viability of pHCs cultured on LEM₁-Dp matrix and col-TCTP was also evaluated using confocal laser microscopy after calcein-AM staining. High fluorescence intensity was observed for the cells cultured in LEM₁-Dp matrix, which suggested that pHCs were viable and healthy up to day 7. Also, an enhanced cell growth from day 2 to day 7 for cell cultured on the matrix was observed (Figure 6d and Supporting Information Figure S8a,b). Z-stacking volume view in confocal microscopy for pHCs cultured on LEM₁-Dp matrix showed a three-dimensional projection of viable cells on days 2, 3, 5, and 7 (Figure 6e and Supporting Information Figure S8c,d).

4.13. Functional Analysis of pHCs Cultured on LEM₁-Dp Matrix. Next, to evaluate the biological functionality of pHCs cultured on LEM₁-Dp matrix, protein expression for albumin and urea secretion studies were carried out. Results of the immunofluorescence study for albumin expression showed that pHCs cultured on both LEM₁-Dp matrix and col-TCTP

expressed albumin, as evidenced by confocal microscopy images (Figure 7a and Supporting Information Figure S9a,b). Also, pHCs cultured on LEM₁-Dp matrix maintained albumin expression for longer periods up to day 7, while it decreased for cells cultured on col-TCTP with time. The qualitative measurements for albumin and urea secretion were carried out by determining their levels in the culture soups. As shown in Figure 6f, the levels of albumin secretion for pHCs cultured on LEM₁-Dp matrix were significantly higher on day 2 and day 7 (44.5 ± 2.12 and $37 \pm 0.07 \mu\text{g}/\text{mL}/(10^6 \text{ cells})$, respectively) as compared to the cells cultured on col-TCTP (9.1 ± 0 and $3.2 \pm 0 \mu\text{g}/\text{mL}/(10^6 \text{ cells})$ for days 2 and 7, respectively), $^{**}p < 0.001$. Similarly, pHCs cultured on LEM₁-Dp matrix showed significantly higher secretion of urea (day 2, $28.1 \pm 0.70 \text{ mg}/\text{dL}/(10^6 \text{ cells})$; day 7, $24.3 \pm 0.56 \text{ mg}/\text{dL}/(10^6 \text{ cells})$) as compared to the cells cultured on col-TCTP (day 2, $12.15 \pm 1.2 \text{ mg}/\text{dL}/(10^6 \text{ cells})$; day 7, $7.85 \pm 3.60 \text{ mg}/\text{dL}/(10^6 \text{ cells})$), $^{**}p < 0.001$ (Figure 6g).

5. DISCUSSION

Maintaining cellular function in a laboratory environment outside the body is a significant challenge for translational research.⁴⁰ Highly specialized cells such as pHCs from liver tissue lose their phenotypic, metabolic and functional characteristics as they are isolated from humans or rodents and seeded onto a standard tissue culture plate.⁴¹ In the past few years, there has been considerable progress in culture techniques to maintain viable and functional hepatocytes but there is a pressing need to explore different biomaterials for long-term cultures of pHCs in vitro.⁴² Large-scale culture of hepatocytes with preserved functions is crucial for biomedical applications such as tissue engineering, drug testing, cell and gene therapy, and extracorporeal liver support systems.

The dipeptide, IΔF was synthesized by solution-phase methods and characterized by RP-HPLC, mass spectroscopy, and infrared spectroscopy. As expected, the IR spectrum of Dp displayed two distinct peaks: at 1691 cm^{-1} (amide-I, $1700\text{--}1600 \text{ cm}^{-1}$, representing C=O stretch accompanied by C–N stretch and N–H bending) and at 1579 cm^{-1} (amide-II, $500\text{--}1600 \text{ cm}^{-1}$ representing C–N stretch accompanied by N–H bending). The peak at 1256 cm^{-1} peak (amide-III region between 1200 and 1350 cm^{-1}) representing N–H in-plane bending accompanied by C–N stretching.⁴³

The dipeptide, IΔF, formed hydrogel under different solvent–buffer systems as indicated by the tube inversion test. 1-Propanol is relatively more biocompatible than methanol; in the present study the hydrogel formed by 1 wt % peptide in 1-propanol–sodium acetate buffer was used in all experiments. CD spectra of Dp at different peptide concentrations showed a strong positive band at 212 nm ,

which suggested the presence of $n-\pi^*$ transitions and random coil-like structures.⁴⁴ An intense negative band at ~ 270 nm could be ascribed to the excitation splitting of the electronic transition of the ΔF chromophore due to the stiff disposition of more than two ΔF residues.⁴⁵ No observable changes in ellipticity with increasing peptide concentration indicated that the peptide did not undergo any major conformational changes during hydrogelation. The process of gelation was also followed by a thioflavin T fluorescence assay. The increase in fluorescence with the increase in peptide concentration indicated that the hydrogelation process was peptide concentration-dependent.

TEM images showed that Dp gel (1 wt %) was an interwoven mesh structure. The presence of unnatural amino acid-like ΔF in the peptide sequence confers resistance to enzymatic degradation.^{12,23,27} Proteolytic stability of the dipeptide gel was tested under different proteolytic conditions and followed by RP-HPLC. Our results showed that the peptide was completely stable in the presence of proteinase K, FBS, and culture supernatants.

To promote the expression of liver-specific functions, LEM was used along with Dp gel to support pHCs culture. The architecture of Dp gel combined with LEM is expected to provide a more suitable microenvironment to hepatic cells similar to native tissues.^{46–49} Decellularized liver showed a complete absence of cellular components and significant removal of the genomic DNA. The LEM composition was further analyzed by mass spectrometry-based proteomic profiling. We were able to identify 149 essential protein components for cell-specific morphology, phenotype, and function, including collagen, elastin, laminin, fibronectin, myosin, keratin, fibrillin, tubulin, and basement proteins, etc.⁵⁰ These findings were similar to those reported earlier.^{37,50}

Solubilization of LEM by pepsin digestion was based on the fact that pepsin cleaves collagen where the three α chains do not form a stable triple-helical structure.^{51,52} The yield of the soluble sLEM was similar to that observed by Half et al.³⁷ Results of 10% SDS page analysis showed that pepsin treatment facilitated the process of LEM solubilization. We mixed sLEM at varying concentrations with 1 wt % Dp gel to make liver-specific functional biomaterial and tested the mechanical strength of the three preparations. The mechanical strength of 1 wt % Dp gel achieved a more favorable stiffness after adding sLEM, although there were no major changes among LEM₁-Dp, LEM₂-Dp, and LEM₃-Dp hybrid matrices. The cellular growth and functions of Huh7 cells on the three hybrid matrices were similar to that observed with TCTP on day 3 of cell cultures. Increasing the sLEM percentage in 1 wt % Dp gel did not lead to any significant enhancement of cellular growth. On the basis of mechanical strength, cell viability, and hepatic functions, we selected LEM₁-Dp matrix for further experiments.

The stability of hydrogel systems plays a crucial role in their development, and therefore mechanical stability of LEM₁-Dp matrix was evaluated using frequency and time sweep rheology studies. Results showed that G' and G'' values were independent of change in angular frequency as well as time, which indicated its high mechanical stability. Fiber diameter plays an important role in cell adhesion to the hydrogels.⁵³ TEM and SEM images showed porous nanofibrillar structures with fiber diameter ~ 200 – 500 nm for LEM₁-Dp matrix. Porous nanofibrillar structures allow the matrix to accommodate a large number of cells and free diffusion of nutrients

and also remove waste materials.⁵⁴ The viability of Huh7 cells cultured on LEM₁-Dp matrix was continuously monitored using light microscopy. Significant improvement in cell viability from day 1 to day 7 was observed in LEM₁-Dp matrix. The cell viability in LEM₁-Dp matrix was similar to that observed in Matrigel which is commonly used as a positive control. Live/dead staining clearly showed that starting from day 2 cell cluster formation was facilitated on the gel surface, indicating strong cell–matrix adhesion. Albumin and urea syntheses by Huh7 cells were 1.8 and 1.44 times higher, respectively, on LEM₁-Dp matrix as compared to Matrigel, suggesting that LEM₁-Dp matrix may be more appropriate than Matrigel for the cellular growth of Huh7 cells. This may be due to the fact that Matrigel lacks major ECM proteins, including fibronectin and type-I collagen, which are essential to facilitate hepatocyte survival and proliferation in the *in vitro* cultures.^{55,56} To investigate if cultured Huh7 cells grew only on the surface or if they invaded deep into the LEM₁-Dp matrix, we obtained confocal Z-stacking images. We found that cells invaded and migrated in LEM₁-Dp matrix into all three (X, Y, Z) planes. Similar three-dimensional growth was also reported for other hydrogels developed for cell culture.²³ The stability of LEM₁-Dp matrix toward proteases present in the culture media of Huh7 cells and pHCs was demonstrated in the overall intact mesh architecture of the LEM₁-Dp matrix on day 7 by SEM.

Following the experiment with the Huh7 cell line, we also investigated the growth of pHCs on LEM₁-Dp matrix. pHCs cultured on LEM₁-Dp matrix showed 3.48 times more cell viability than col-TCTP. For pHC culture, col-TCTP has been widely used by researchers.⁵⁷ pHCs cultured on LEM₁-Dp matrix maintained viability, morphology, and functionality up to day 7. pHCs cultured on LEM₁-Dp matrix exhibited 11.56 times higher albumin secretion and 3.09 times urea production on day 7 than the col-TCTP. This suggested that the LEM-based hydrogel has the ability to preserve hepatocyte functions in culture better than col-TCTP alone. In an earlier study, Wang et al. also demonstrated that hepatocytes cultured on the PuraMatrix scaffold secrete higher albumin and urea than those on collagen sandwich cultures.⁵⁸ Immunofluorescence stain of albumin showed pHCs on the hybrid matrix maintained hepatic functions until day 7, whereas the functions of pHCs started declining on col-TCTP after day 2. Z-stacking of confocal laser microscopy volume view also clearly indicated pHCs seeded on top of the hydrogel migrated into its interior within 5 days. The surface morphology of the hepatocyte changed to a bumpy surface with distinguishable individual pHCs on day 7. Similar observations have been reported on hepatocyte aggregates earlier.⁵⁹ Overall, the above results suggest that LEM₁-Dp hybrid matrix is highly suitable for *in vitro* culture of primary hepatocytes.

6. CONCLUSION

In conclusion, the present study has shown that the hybrid hydrogel, consisting of a modified dipeptide-based hydrogel and solubilized LEM, provides a 3D scaffold and appropriate microenvironment for pHCs culture. Solubilization, characterization, and suitability of LEM for supporting the 3D culture of pHCs have been described earlier. Proteomic analysis of LEM used in this study showed it to be similar to earlier described LEM-based preparations. The mechanical strength of the hybrid hydrogel was also comparable to the liver extracellular matrix described in the literature. Given that the dipeptide hydrogel is easy to prepare, stable to proteolytic degradation,

and highly biocompatible may offer a good alternative for further development for in vitro pHCs culture applications.

■ ASSOCIATED CONTENT

SI Supporting Information

The Supporting Information is available free of charge at <https://pubs.acs.org/doi/10.1021/acsabm.2c00526>.

1ΔF azlactone synthesis; infrared spectrum; LC/MS-MS data; Dp gelation; CD spectra; thioflavin T fluorescence assay; RP-HPLC; amplitude, frequency, and time sweeps; SEM of LEM₁-Dp matrix stability; confocal laser microscopy images; bright-field microscopy images; confocal microscopy analysis (PDF)

■ AUTHOR INFORMATION

Corresponding Authors

Virander Singh Chauhan – International Centre for Genetic Engineering and Biotechnology, New Delhi, Delhi 110067, India; orcid.org/0000-0001-9875-9549; Email: viranderschauhan@gmail.com

Savneet Kaur – Institute of Liver and Biliary Sciences, New Delhi, Delhi 110070, India; Email: savykaur@gmail.com

Authors

Saikat Biswas – International Centre for Genetic Engineering and Biotechnology, New Delhi, Delhi 110067, India;

orcid.org/0000-0002-9667-678X

Ashwini Vasudevan – Institute of Liver and Biliary Sciences, New Delhi, Delhi 110070, India

Nitin Yadav – International Centre for Genetic Engineering and Biotechnology, New Delhi, Delhi 110067, India

Saurabh Yadav – International Centre for Genetic Engineering and Biotechnology, New Delhi, Delhi 110067, India

Preeti Rawal – Institute of Liver and Biliary Sciences, New Delhi, Delhi 110070, India

Impreet Kaur – Institute of Liver and Biliary Sciences, New Delhi, Delhi 110070, India

Dinesh M. Tripathi – Institute of Liver and Biliary Sciences, New Delhi, Delhi 110070, India

Complete contact information is available at:

<https://pubs.acs.org/doi/10.1021/acsabm.2c00526>

Notes

The authors declare no competing financial interest.

■ ACKNOWLEDGMENTS

This study was funded by the Department of Biotechnology, Government of India (BT/PR2573/NNT/28/534/2011), Department of Science and Technology, India, DST-ASEAN Grant (CRD/2019/000120), and Science and Engineering Research Board, India (SRG/2019/002128). We also acknowledge the Department of Science and Technology, Government of India (SB/S2/JCB-41/2014), Department of Biotechnology, Government of India (BT/HRD/35/07/VSC/2015), and BIRAC, Government of India (BIRAC/CCAMP0770/BIG-13/18) for financial support. We are really thankful to Dr. Paushali Mukherjee for her valuable suggestion for primary hepatocyte culture. We also thank Mrs. Purnima Kumari, Mrs. Tenzin Choedon, and Indu Sharma for their assistance in confocal microscopy, transmission electron microscopy, and pHCs isolation, respectively, and Dr. Jaswinder Singh Maras, Mr. Babu Mathew P, and Mr. Suneet Shekhar Singh for the

cooperation during mass spectrometry. We thank Dr. S. Swaminathan and Mr. Budharaju Harshavardhan for their help in the rheology experiment. A few infographics of graphical art were created with BioRender.com.

■ ABBREVIATIONS USED:

CD, circular dichroism
DLS, dynamic light scattering
Dp, dipeptide
FBS, Fetal bovine serum
FT-IR, Fourier transform infrared
LEM, liver extracellular matrix
PBS, phosphate buffered saline
pHCs, primary hepatocytes
RP-HPLC, reverse-phase high-performance liquid chromatography
SEM, scanning electron microscopy
TEM, transmission electron microscopy
ΔF, α,β -dehydrophenylalanine

■ REFERENCES

- (1) Trefts, E.; Gannon, M.; Wasserman, D. H. The liver. *Curr. Biol.* **2017**, *27* (21), R1147–R1151.
- (2) Asrani, S. K.; Devarbhavi, H.; Eaton, J.; Kamath, P. S. Burden of liver diseases in the world. *J. Hepatol.* **2019**, *70* (1), 151–171.
- (3) Nostedt, J. J.; Shapiro, J.; Freed, D. H.; Bigam, D. L. Addressing organ shortages: progress in donation after circulatory death for liver transplantation. *Can. J. Surg.* **2020**, *63* (2), E135–E141.
- (4) Cardoso, L. M. D. F.; Moreira, L. F. P.; Pinto, M. A.; Henriques-Pons, A.; Alves, L. A. Domino Hepatocyte Transplantation: A Therapeutic Alternative for the Treatment of Acute Liver Failure. *Can. J. Gastroenterol. Hepatol.* **2018**, *2018*, 2593745.
- (5) Li, H.; Chen, H. S. H.; Nyberg, S. L. Extracorporeal Liver Support and Liver Transplant for Patients with Acute-on-Chronic Liver Failure. *Semin. Liver Dis.* **2016**, *36* (2), 153–60.
- (6) Iansante, V.; Mitry, R. R.; Filippi, C.; Fitzpatrick, E.; Dhawan, A. Human hepatocyte transplantation for liver disease: current status and future perspectives. *Pediatr. Res.* **2018**, *83* (1–2), 232–240.
- (7) Tricot, T.; De Boeck, J.; Verfaillie, C. Alternative Cell Sources for Liver Parenchyma Repopulation: Where Do We Stand? *Cells* **2020**, *9* (3), 566.
- (8) Afshari, A.; Shamdani, S.; Uzan, G.; Naserian, S.; Azarpira, N. Different approaches for transformation of mesenchymal stem cells into hepatocyte-like cells. *Stem Cell Res. Ther.* **2020**, *11* (1), 54.
- (9) Ruoß, M.; Vosough, M.; Königsrainer, A.; Nadalin, S.; Wagner, S.; Sajadian, S.; Huber, D.; Heydari, Z.; Ehnert, S.; Hengstler, J. G.; Nussler, A. K. Towards improved hepatocyte cultures: Progress and limitations. *Food Chem. Toxicol.* **2020**, *138*, 111188.
- (10) Lee, K. Y.; Mooney, D. J. Hydrogels for tissue engineering. *Chem. Rev.* **2001**, *101* (7), 1869–79.
- (11) Reddy, M. S. B.; Ponnamm, D.; Choudhary, R.; Sadasivuni, K. K. A Comparative Review of Natural and Synthetic Biopolymer Composite Scaffolds. *Polymers* **2021**, *13* (7), 1105.
- (12) Thota, C. K.; Yadav, N.; Chauhan, V. S. A novel highly stable and injectable hydrogel based on a conformationally restricted ultrashort peptide. *Sci. Rep.* **2016**, *6*, 31167.
- (13) Black, K. A.; Lin, B. F.; Wonder, E. A.; Desai, S. S.; Chung, E. J.; Ulery, B. D.; Katari, R. S.; Tirrell, M. V. Biocompatibility and characterization of a peptide amphiphile hydrogel for applications in peripheral nerve regeneration. *Tissue Eng. Part A* **2015**, *21* (7–8), 1333–42.
- (14) Saini, A.; Chauhan, V. S. Self-assembling properties of peptides derived from TDP-43 C-terminal fragment. *Langmuir* **2014**, *30* (13), 3845–56.
- (15) Wu, J.; Mari-Buy, N.; Muinos, T. F.; Borros, S.; Favia, P.; Semino, C. E. Nanometric self-assembling peptide layers maintain

adult hepatocyte phenotype in sandwich cultures. *J. Nanobiotechnol.* **2010**, *8*, 29.

(16) Zhou, M.; Smith, A. M.; Das, A. K.; Hodson, N. W.; Collins, R.; Ulijn, R. V.; Gough, J. E. Self-assembled peptide-based hydrogels as scaffolds for anchorage-dependent cells. *Biomaterials*. **2009**, *30* (13), 2523–30.

(17) Panda, J. J.; Chauhan, V. S. Short peptide based self-assembled nanostructures: implications in drug delivery and tissue engineering. *Polym. Chem.* **2014**, *5*, 4418–4436.

(18) Yadav, N.; Chauhan, M. K.; Chauhan, V. S. Short to ultrashort peptide-based hydrogels as a platform for biomedical applications. *Biomater. Sci.* **2020**, *8* (1), 84–100.

(19) de Groot, N. S.; Parella, T.; Aviles, F. X.; Vendrell, J.; Ventura, S. Ile-Phe dipeptide self-assembly: clues to amyloid formation. *Biophys. J.* **2007**, *92* (5), 1732–1741.

(20) Bellotto, O.; Kralj, S.; Melchionna, M.; Pengo, P.; Kisovec, M.; Podobnik, M.; De Zorzi, R. D.; Marchesan, S. Self-Assembly of Unprotected Dipeptides into Hydrogels: Water-Channels Make the Difference. *ChemBioChem* **2022**, *23* (2), e202100518.

(21) Mendel, D.; Ellman, J. A.; Chang, Z.; Veenstra, D. L.; Kollman, P. A.; Schultz, P. G. Probing protein stability with unnatural amino acids. *Science* **1992**, *256* (5065), 1798–802.

(22) Adessi, C.; Soto, C. Converting a peptide into a drug: strategies to improve stability and bioavailability. *Curr. Med. Chem.* **2002**, *9* (9), 963–78.

(23) Panda, J. J.; Dua, R.; Mishra, A.; Mittra, B.; Chauhan, V. S. 3D cell growth and proliferation on a RGD functionalized nanofibrillar hydrogel based on a conformationally restricted residue containing dipeptide. *ACS Appl. Mater. Interfaces* **2010**, *2* (10), 2839–48.

(24) Gupta, M.; Bagaria, A.; Mishra, A.; Mathur, P.; Basu, A.; Ramakumar, S.; Chauhan, V. S. Self-Assembly of a Dipeptide-Containing Conformationally Restricted Dehydrophenylalanine Residue to Form Ordered Nanotubes. *Adv. Mater.* **2007**, *19*, 858–861.

(25) Panda, J. J.; Mishra, A.; Basu, A.; Chauhan, V. S. Stimuli responsive self-assembled hydrogel of a low molecular weight free dipeptide with potential for tunable drug delivery. *Biomacromolecule* **2008**, *9* (8), 2244–50.

(26) Panda, J. J.; Kaul, A.; Kumar, S.; Alam, S.; Mishra, A. K.; Kundu, G. C.; Chauhan, V. S. Modified dipeptide-based nanoparticles: vehicles for targeted tumor drug delivery. *Nanomedicine* **2013**, *8* (12), 1927–42.

(27) Mishra, A.; Panda, J. J.; Basu, A.; Chauhan, V. S. Nanovesicles based on self-assembly of conformationally constrained aromatic residue containing amphiphilic dipeptides. *Langmuir* **2008**, *24* (9), 4571–6.

(28) Panda, J. J.; Kaul, A.; Alam, S.; Babbar, A. K.; Mishra, A. K.; Chauhan, V. S. Designed peptides as model self-assembling nanosystems: characterization and potential biomedical applications. *Ther. Delivery* **2011**, *2* (2), 193–204.

(29) Varshney, A.; Panda, J. J.; Singh, A. K.; Yadav, N.; Bihari, C.; Biswas, S.; Sarin, S. K.; Chauhan, V. S. Targeted delivery of microRNA-199a-3p using self-assembled dipeptide nanoparticles efficiently reduces hepatocellular carcinoma in mice. *Hepatology* **2018**, *67* (4), 1392–1407.

(30) Verma, P.; Biswas, S.; Yadav, N.; Khatri, A.; Siddiqui, H.; Panda, J. J.; Rawat, B. S.; Tailor, P.; Chauhan, V. S. Delivery of a Cancer-Testis Antigen-Derived Peptide Using Conformationally Restricted Dipeptide-Based Self-Assembled Nanotubes. *Mol. Pharmaceutics* **2021**, *18* (10), 3832–3842.

(31) Anand, G.; Biswas, S.; Yadav, N.; Mukherjee, P.; Chauhan, V. S. Production and Immunogenicity of a Tag-Free Recombinant Chimera Based on PfMSP-1 and PfMSP-3 Using Alhydrogel and Dipeptide-Based Hydrogels. *Vaccines* **2021**, *9* (7), 782.

(32) Khatri, A.; Mishra, A.; Chauhan, V. S. Characterization of DNA Condensation by Conformationally Restricted Dipeptides and Gene Delivery. *J. Biomed. Nanotechnol.* **2017**, *13* (1), 35–53.

(33) Alam, S.; Panda, J. J.; Chauhan, V. S. Novel dipeptide nanoparticles for effective curcumin delivery. *Int. J. Nanomed.* **2012**, *7*, 4207–4222.

(34) Loneker, A. E.; Faulk, D. M.; Hussey, G. S.; D'Amore, A.; Badylak, S. F. Solubilized liver extracellular matrix maintains primary rat hepatocyte phenotype in-vitro. *J. Biomed. Mater. Res. A* **2016**, *104* (4), 957–65.

(35) Lee, J. S.; Shin, J.; Park, H. M.; Kim, Y. G.; Kim, B. G.; Oh, J. W.; Cho, S. W. Liver extracellular matrix providing dual functions of two-dimensional substrate coating and three-dimensional injectable hydrogel platform for liver tissue engineering. *Biomacromolecules* **2014**, *15* (1), 206–18.

(36) Sharma, A.; Rawal, P.; Tripathi, D. M.; Alodiya, D.; Sarin, S. K.; Kaur, S.; Ghosh, S. Upgrading Hepatic Differentiation and Functions on 3D Printed Silk-Decellularized Liver Hybrid Scaffolds. *ACS Biomater. Sci. Eng.* **2021**, *7* (8), 3861–3873.

(37) Coronado, R. E.; Somarakis-Cormier, M.; Natesan, S.; Christy, R. J.; Ong, J. L.; Halff, G. A. Decellularization and Solubilization of Porcine Liver for Use as a Substrate for Porcine Hepatocyte Culture: Method Optimization and Comparison. *Cell Transplant.* **2017**, *26* (12), 1840–1854.

(38) Yadav, N.; Chauhan, M. K.; Chauhan, V. S. Conformationally constrained dipeptide-based hydrogel as a platform for 3D cell growth and tissue engineering applications. *Appl. Nanosci.* **2021**, *11*, 2019–2031.

(39) Tripathi, D. M.; Rohilla, S.; Kaur, I.; Siddiqui, H.; Rawal, P.; Juneja, P.; Kumar, V.; Kumari, A.; Naidu, V. G. M.; Ramakrishna, S.; Banerjee, S.; Puria, R.; Sarin, S. K.; Kaur, S. Immunonano-Lipocarrier-Mediated Liver Sinusoidal Endothelial Cell-Specific RUNX1 Inhibition Impedes Immune Cell Infiltration and Hepatic Inflammation in Murine Model of NASH. *Int. J. Mol. Sci.* **2021**, *22* (16), 8489.

(40) Brooks, S. M.; Alper, H. S. Applications, challenges, and needs for employing synthetic biology beyond the lab. *Nat. Commun.* **2021**, *12* (1), 1390.

(41) Castell, J. V.; Jover, R.; Martinez-Jimenez, C. P.; Gmez-Lechn, M. J. Hepatocyte cell lines: their use, scope and limitations in drug metabolism studies. *Expert Opin. Drug Metab. Toxicol.* **2006**, *2* (2), 183–212.

(42) Hosseini, V.; Maroufi, N. F.; Saghati, S.; Asadi, N.; Darabi, M.; Ahmad, S. N. S.; Hosseinkhani, H.; Rahbarghazi, R. Current progress in hepatic tissue regeneration by tissue engineering. *J. Transl. Med.* **2019**, *17* (1), 383.

(43) Singh, B. R. Basic Aspects of the Technique and Applications of Infrared Spectroscopy of Peptides and Proteins. *Infrared Analysis of Peptides and Proteins*; ACS Symposium Series, Vol. 750; American Chemical Society: Washington, DC, 1999; Chapter 1, pp 2–37..

(44) Ranjbar, B.; Gill, P. Circular Dichroism Techniques: Biomolecular and Nanostructural Analyses- A Review. *Chem. Biol. Drug Des.* **2009**, *74*, 101–120.

(45) Skelton, N. J.; Blandl, T.; Russell, S. J.; Starovasnik, M. A.; Cochran, A. G. β -hairpin polypeptides by design and selection. *J. Spectrosc.* **2003**, *17*, 148024.

(46) Lang, R.; Stern, M. M.; Smith, L.; Liu, Y.; Bharadwaj, S.; Liu, G.; Baptista, P. M.; Bergman, C. R.; Soker, S.; Yoo, J. J.; Atala, A.; Zhang, Y. Three-dimensional culture of hepatocytes on porcine liver tissue-derived extracellular matrix. *Biomaterials* **2011**, *32* (29), 7042–52.

(47) Uygun, B. E.; Soto-Gutierrez, A.; Yagi, H.; Izamis, M.-L.; Guzzardi, M. A.; Shulman, C.; Milwid, J.; Kobayashi, N.; Tilles, A.; Berthiaume, F.; Hertl, M.; Nahmias, Y.; Yarmush, M. L.; Uygun, K. Organ reengineering through development of a transplantable recellularized liver graft using decellularized liver matrix. *Nat. Med.* **2010**, *16* (7), 814–620.

(48) Nakamura, S.; Ijima, H. Solubilized matrix derived from decellularized liver as a growth factor-immobilizable scaffold for hepatocyte culture. *J. Biosci. Bioeng.* **2013**, *116* (6), 746–53.

(49) Bual, R.; Kimura, H.; Ikegami, Y.; Shirakigawa, N.; Ijima, H. Fabrication of liver-derived extracellular matrix nanofibers and functional evaluation in vitro culture using primary hepatocytes. *Materialia* **2018**, *4*, 518–528.

(50) Klaas, M.; Kangur, T.; Viil, J.; Maemets-Allas, K.; Minajeva, A.; Vadi, K.; Antsov, M.; Lapidus, N.; Jarvekulg, M.; Jaks, V. The

alterations in the extracellular matrix composition guide the repair of damaged liver tissue. *Sci. Rep.* **2016**, *6*, 27398.

(51) Alevra Sarika, N.; Payen, V. L.; Fleron, M.; Ravau, J.; Brusa, D.; Najimi, M.; De Pauw, E.; Eppe, G.; Mazzucchelli, G.; Sokal, E. M.; des Rieux, A.; El Taghdouini, A. Human Liver-Derived Extracellular Matrix for the Culture of Distinct Human Primary Liver Cells. *Cells* **2020**, *9* (6), 1357.

(52) Bual, R. P.; Ijima, H. Intact extracellular matrix component promotes maintenance of liver-specific functions and larger aggregates formation of primary rat hepatocytes. *Regen. Ther.* **2019**, *11*, 258–268.

(53) Keun Kwon, I.; Kidoaki, S.; Matsuda, T. Electrospun nano- to microfiber fabrics made of biodegradable copolyesters: structural characteristics, mechanical properties and cell adhesion potential. *Biomaterials* **2005**, *26* (18), 3929–3939.

(54) Mandal, S.; Dube, T.; Mohapatra, A. K.; Choudhury, S.; Khanam, F.; Yadav, P.; Chauhan, V. S.; Mishra, J.; Panda, J. J. Engineered Biocompatible and Stable Dipeptide Hydrogel with Tunable Mechanical and Cell Growth Properties to Embolden Neuroglial Cell Growth. *Int. J. Pept. Res. Ther.* **2021**, *27*, 2795–2808.

(55) Kaur, S.; Kaur, I.; Rawal, P.; Tripathi, D. M.; Vasudevan, A. Non-matrigel scaffolds for organoid cultures. *Cancer Lett.* **2021**, *504*, 58–66.

(56) Kato, S.; Otsu, K.; Ohtake, K.; Kimura, Y.; Yashiro, T.; Suzuki, T.; Akamatsu, N. Concurrent changes in sinusoidal expression of laminin and affinity of hepatocytes to laminin during rat liver regeneration. *Exp. Cell Res.* **1992**, *198* (1), 59–68.

(57) Parenteau-Bareil, R.; Gauvin, R.; Berthod, F. Collagen-Based Biomaterials for Tissue Engineering Applications. *Materials* **2010**, *3* (3), 1863–1887.

(58) Wang, S.; Nagrath, D.; Chen, P. C.; Berthiaume, F.; Yarmush, M. L. Three-dimensional primary hepatocyte culture in synthetic self-assembling peptide hydrogel. *Tissue Eng. Part A* **2008**, *14* (2), 227–36.

(59) Tseng, T. C.; Wong, C. W.; Hsieh, F. Y.; Hsu, S. H. Biomaterial Substrate-Mediated Multicellular Spheroid Formation and Their Applications in Tissue Engineering. *Biotechnol. J.* **2017**, *12* (12), 1700064.

Recommended by ACS

Development of a 3D Cell Culture System Using Amphiphilic Polydepsipeptides and Its Application to Hepatic Differentiation

Junko Enomoto, Hayato Matsui, *et al.*

SEPTEMBER 08, 2021
ACS APPLIED BIO MATERIALS

READ 

Mimicking Physiologically Relevant Hepatocyte Zonation Using Immunomodulatory Silk Liver Extracellular Matrix Scaffolds toward a Bioartificial Liver Platform

G. Janani and Biman B. Mandal

MAY 21, 2021
ACS APPLIED MATERIALS & INTERFACES

READ 

Integration of Primary Endocrine Cells and Supportive Cells Using Functionalized Silk Promotes the Formation of Prevascularized Islet-like Clusters

Ulrika Johansson, My Hedhammar, *et al.*

DECEMBER 30, 2019
ACS BIOMATERIALS SCIENCE & ENGINEERING

READ 

Hydrogel-Supported, Engineered Model of Vocal Fold Epithelium

Anitha Ravikrishnan, Xinqiao Jia, *et al.*

FEBRUARY 26, 2021
ACS BIOMATERIALS SCIENCE & ENGINEERING

READ 

Get More Suggestions >